# Novel Class of Quinone-Bearing Polyamines as Multi-Target-Directed Ligands To Combat Alzheimer's Disease

Maria Laura Bolognesi,*,† Rita Banzi,† Manuela Bartolini,† Andrea Cavalli,† Andrea Tarozzi,‡ Vincenza Andrisano,† Anna Minarini,† Michela Rosini,† Vincenzo Tumiatti,† Christian Bergamini,§ Romana Fato,§ Giorgio Lenaz,§ Patrizia Hrelia,‡ Antonino Cattaneo,|| Maurizio Recanatini,† and Carlo Melchiorre*,†

*Department of Pharmaceutical Sciences, Alma Mater Studiorum, University of Bologna, Via Belmeloro 6, and Departments of Biochemistry and Pharmacology, Alma Mater Studiorum, University of Bologna, Via Irnerio 48, 40126 Bologna, and Lay Line Genomics, Via di Castel Romano 100, 00128 Rome, Italy*

*Received May 14, 2007*

One of the characteristics of Alzheimer's disease (AD) that hinders the discovery of effective disease-modifying therapies is the multifactorial nature of its etiopathology. To circumvent this drawback, the use of multi-target-directed ligands (MTDLs) has recently been proposed as a means of simultaneously hitting several targets involved in the development of the AD syndrome. In this paper, a new class of MTDLs based on a polyamine−quinone skeleton, whose lead (memoquin, **2**) showed promising properties in preclinical investigations (Cavalli et al. *Angew. Chem., Int. Ed.* **2007**, *46*, 3689−3692), is described. **3**−**29** were tested in vitro against a number of isolated AD-related targets, namely, AChE and BChE, and A$\beta$ aggregation (both AChE-mediated and self-induced). Furthermore, the ability of the compounds to counteract the oxidative stress in a human neuronal-like cellular system (SH-SY5Y cells) was assayed, in both the presence and absence of NQO1, an enzyme able to generate and maintain the reduced form of quinone.

## Introduction

Treating Alzheimer's disease (AD[a]) remains a challenge for the pharmaceutical community. Despite intensive study, its molecular etiology is still enigmatic, and although a variety of drug treatments have been shown to benefit patients, none represent a real cure. On the basis of the so-called cholinergic hypothesis,[1,2] a new generation of acetylcholinesterase inhibitors (AChEIs) were developed and marketed in the 1990s to specifically treat AD. These were joined in 2004 by memantine, an NMDA receptor antagonist.[3] AChEIs, although valuable in restoring cholinergic dysfunction and in improving the patient's quality of life, have revealed themselves to be of limited effect, suitable only for palliative use. In more recent times, mechanism-based approaches directed toward two proteins, amyloid-$\beta$ (A$\beta$)[4] and $\tau$,[5] have become a major focus of research. A$\beta$ is the major constituent of amyloid plaques, one of the key pathological characteristics of AD, while phosphorylated $\tau$ is the main component of neurofibrillary tangles, the second major characterizing factor for AD.[6] However, no new molecules interfering with the biochemical pathways of either A$\beta$ or $\tau$ have so far reached the market. The reason for this drawback appears to reside in the fact that, like many common diseases, AD is multifactorial in origin, with both genetic and environmental contributions likely to play an important role in the pathogenesis. Accordingly, the quest for new and disease-modifying agents could be addressed by shifting the drug discovery paradigm from mono- to multi-target-directed ligands (MTDLs), which are more adequate for addressing the complexity of the disease. In this regard, recent results obtained with MTDLs, i.e., single chemical entities able to hit distinct molecular targets in the neurodegenerative cascade, have been encouraging,[7−10] convincing us that they might represent the best pharmacological option for tackling the multifactorial nature of AD and for stopping the disease progression.[11,12]

With these concepts in mind, we initiated a research program aimed at identifying new MTDLs possessing different activities toward AD-relevant targets, such as acetylcholinesterase (AChE), A$\beta$ processing and aggregation, and oxidative stress. Indeed, oxidative damage is retained as one of the major pathogenic mechanisms in AD, and since it occurs early in the pathogenesis,[13] it represents an ideal target for intervention.

Although a few medicinal chemistry strategies have so far been developed to create MTDLs by joining functionally distinct pharmacophores,[14] the design of MTDLs is a complex task. Clearly, the success rate can be greatly increased by properly selecting the starting scaffold: conceptually, it would appear that the lack of tight molecular specificity for only one given target may represent a prerequisite for the choice of a better lead compound. In this respect, some years ago we postulated that polyamines represent a universal template, able to interact with all protein targets, whose affinity for a target can be modulated by (a) inserting appropriate substituents on the nitrogen atoms and (b) altering the chain length separating the amine functions to fit the distance between the carboxylate or aromatic residues of the biological counterpart.[15,16]

We therefore started from a set of polyamine derivatives that already showed a dual action, being both AChEIs and muscarinic $M_2$ receptor antagonists,[17] and planned to modify their structure by incorporating into their backbone an antioxidant function. Among the possible carriers of radical scavenger activity, attention was focused on the benzoquinone fragment of coenzyme Q10 (CoQ), as this natural antioxidant offered promise against AD both in vitro[18] and in vivo.[19] Moreover,

* To whom correspondence should be addressed. Phone +39 0512099700. Fax: +39 0512099734. E-mail: marialaura.bolognesi@unibo.it (M.L.B.); carlo.melchiorre@unibo.it (C.M.).

† Department of Pharmaceutical Sciences, University of Bologna.

‡ Department of Pharmacology, University of Bologna.

§ Department of Biochemistry, University of Bologna.

|| Lay Line Genomics.

[a] Abbreviations: A$\beta$, amyloid-$\beta$; AChE, acetylcholinesterase; AChEI, acetylcholinesterase inhibitor; AD, Alzheimer's disease; APP, amyloid precursor protein; BACE-1, $\beta$-secretase; BChE, butyrylcholinesterase; CoQ, coenzyme Q10; MD, molecular dynamics; MTDL, multi-target-directed ligand; NQO1, NAD(P)H:quinone oxidoreductase 1; PAS, peripheral anionic site; ROS, reactive oxygen species; SAR, structure−activity relationship.

10.1021/jm070559a CCC: $37.00 
Published on Web 09/13/2007

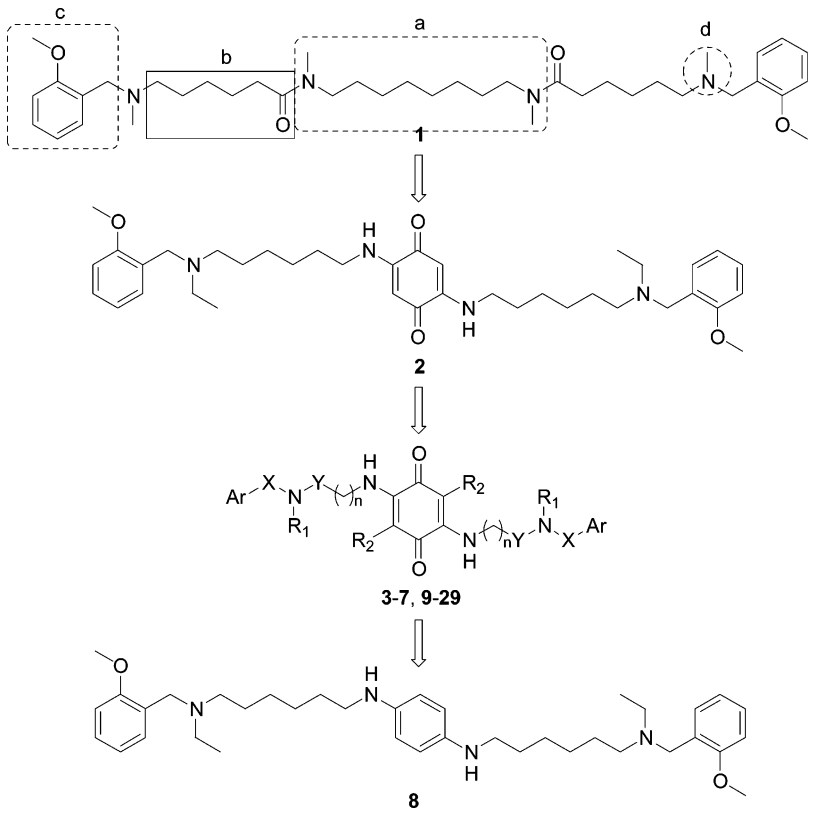


**Figure 1.** Design strategy for compounds **2**−**29**. The lead compound **1** (caproctamine) was modified to afford compounds **2**−**7** and **9**−**29** by replacing (a) the inner octamethylene spacer with a 3,6-(un)substituted 2,5-diamino-1,4-benzoquinone to introduce a group with antioxidant properties and reduced flexibility, (b) the hexamethylene spacer between inner and outer nitrogen atoms with different chain lengths to verify the importance, if any, of the distance between the nitrogen atoms and the terminal aryl groups, (c) the 2-methoxybenzyl moiety with differently substituted benzyl and phenethyl groups to assess the role of the aromatic ring and its substituents and of the distance of the ring from the outer nitrogen atoms as well, and (d) the methyl group with different moieties to optimize the activity. Finally, the 1,4-benzoquinone moiety of **2** was replaced with a phenyl ring, affording **8**, to verify the importance of such a functionality to the biological profile. See Table 1 for the chemical structure of compounds **2**−**7** and **9**−**29**.

CoQ and different benzoquinone derivatives have been shown to modulate AD molecular targets, directly inhibiting A$\beta$ aggregation.[20,21]

As a first approach to convert these AChEIs into MTDLs, the insertion of an antioxidant moiety into the polyamine backbone was investigated. Detailed structure−activity relationship (SAR) and docking studies have revealed that, in AChE, the biophoric space around the octamethylene spacer separating the two amide functions of **1** (caproctamine) is quite "tolerant" and can accommodate a variety of cyclic moieties.[22] We therefore decided to introduce the benzoquinone nucleus to replace the inner polymethylene chain (see Figure 1 for the design strategy). Moreover, in the resulting prototypic structure 2,5-bis(diamino)-1,4-benzoquinone **2** (memoquin),[23] the two nitrogen atoms in positions 2 and 5 of the benzoquinone moiety are amide-like in character, precisely mimicking the amide bonds of **1**. Due to a resonance effect, a hydrophobic and planar $\pi$ system is generated, which is able, in principle, to bind A$\beta$ and to perturb protein−protein interactions in the fibrillogenesis process.[24]

On this basis, **2** was developed with the aim of obtaining an MTDL effective on different biochemical cascades relevant for AD pathology. As reported elsewhere,[23] not only did this compound show high AChE inhibitory activity, but it also proved to be an inhibitor of the amyloid precursor protein (APP) processing enzyme $\beta$-secretase (BACE-1). It was also able to block in vitro A$\beta$ aggregation mediated by AChE, together with oxidative processes. In vivo, **2** showed the ability to rescue scopolamine-induced amnesia in mice. Moreover, it caused an effective recovery from the cholinergic deficit, $\tau$ hyperphosphorylation, A$\beta$ deposition, and behavioral abnormalities in AD11 anti-NGF mice, a comprehensive transgenic model of AD.

However, systematic modifications of **2** to design more effective ligands have not been reported so far. To clarify the importance of the polyamine side chain and the quinone functionality for the different activities relevant for AD, a chemical modification of **2** was performed, affording compounds **3**−**29** according to the design strategy as outlined in Figure 1.

In the present paper, we delineate both the general SARs and unique multiple mechanism of action of these novel MTDLs as determined by a number of different in vitro assays accounting for AChE inhibition, A$\beta$ aggregation, and antioxidant effects. The SAR for BACE-1 inhibition and a complete account of the in vivo actions will be reported in separate papers.

## Chemistry

The key intermediates for the synthesis of **2**−**13** and **16**−**29** were the *N*,*N*-disubstituted diamines **65**−**83** (Scheme 1). The introduction of the aryl moiety on the terminal free amine function of the commercially available *N*-Z-1,$\omega$-diaminoalkanes was performed through condensation with the appropriate aryl aldehyde and subsequent reduction of the intermediate Schiff bases with $NaBH_4$ to give **30**−**46**. Initially, *N*-ethylation of **30**−**38** to afford **47**−**55** was achieved with diethyl sulfate. The strategy depicted in Scheme 1 was suitable for our initial purposes. However, in view of the need to produce a certain

**Scheme 1.** Synthesis of Diamines **65**−**83** and of Quinone-Bearing Polyamines **2**−**7**[a]

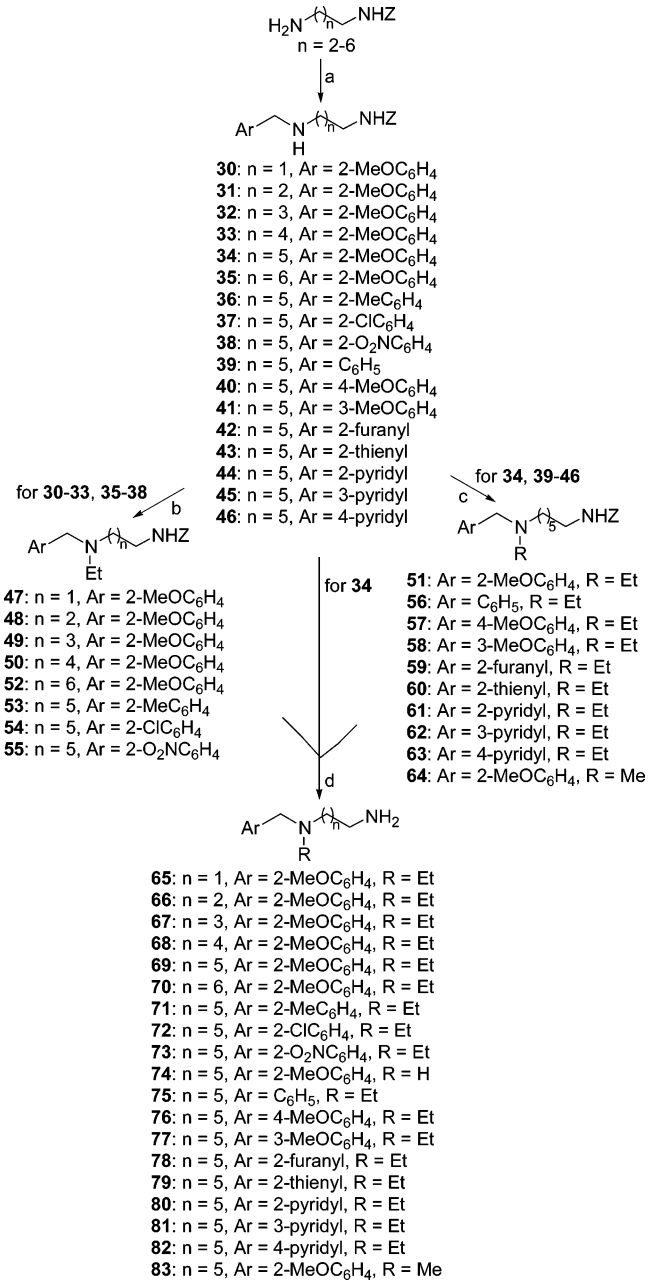


[a] Reagents and conditions: Z = $C_6H_5CH_2OCO-$; (a) ArCHO, toluene, Dean−Stark trap, reflux, 6 h, then $NaBH_4$, EtOH, rt, overnight; (b) diethyl sulfate, toluene, reflux, 6 h, then rt, overnight; (c) for **34** to give **51**, $CH_3CHO$, $NaBH_3CN$, MeOH, rt, overnight; for **39**−**46** to give **56**−**63**, AcOH, $NaBH_4$, THF, 60 °C, 4 h; for **34** to give **64**, HCOOH, HCHO, $H_2O$, reflux, 6 h; (d) 30% HBr, AcOH, rt, overnight.

amount of the final compounds, such as **2**, for in vivo biological testing and to create a library of compounds to expedite broad SAR studies within this structural class of quinone-bearing polyamines, the procedure had a number of undesirable characteristics. In particular, a challenging step in Scheme 1 was the ethylation of the benzylic amino group of, for example, **34**. When the reaction was performed on a 100 mg scale with diethyl sulfate in toluene at 80 °C, the corresponding compound **51** was obtained in 75% yield. However, various byproducts, such as quaternary ammonium cations, were produced when the scale was increased to multigrams. As expected, these were very difficult to separate from the desired **51** (yield estimated to be less than 20%), even by repeated crystallization of the

**Scheme 2.** Synthesis of Diamine **85**[a]

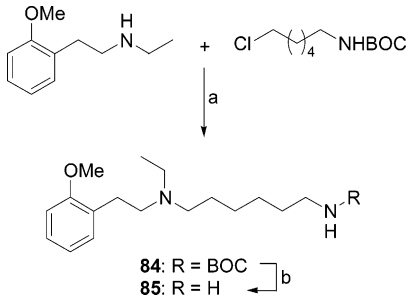


[a] Reagents and conditions: BOC = $Me_3COCO-$; (a) DMF, KI, $Et_3N$, 105 °C, 48 h; (b) $CF_3COOH$, $CHCl_3$, rt, 2 h.

**Scheme 3.** Synthesis of Amine Amide **87**[a]

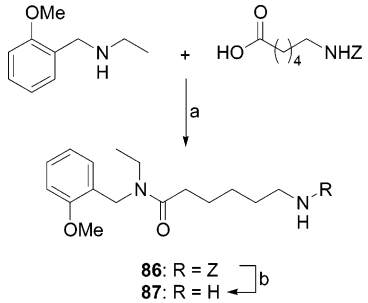


[a] Reagents and conditions: Z = $C_6H_5CH_2OCO-$; (a) EtOCOCl, $Et_3N$, dioxane, rt, 12 h; (b) $H_2$, Pd/C, MeOH, rt,1 h.

corresponding salts or by silica gel chromatography, although the latter technique is not realistic for large-scale purification. Therefore, for compounds **39**−**46**, a reductive amination protocol with $CH_3COOH$ and $NaBH_4$ in THF was used,[25] leading to **56**−**63** with higher yields. This reaction does not usually work on substrates carrying substituents in the 2 position of the aromatic ring. Thus, in the case of **34**,[23] the standard Borch reductive amination approach was used, which afforded **51** in 50% yield, employing washings as a purification step. Eschweiler−Clarke methylation of **34** gave the methyl derivative **64**. Removal of the protecting group of **47**−**64** in acidic medium gave the desired synthons **65**−**83**.

Due to the different reactivities and availabilities of the starting materials, slightly modified procedures were followed for the preparation of intermediates **85**, **87**, and **90** (Schemes 2−4). For **85**, *N*-ethyl-*N*-(2-methoxy)phenethylamine[26] was alkylated with (6-chlorohexyl)carbamic acid *tert*-butyl ester[27] to afford **84**, which was treated with $CF_3COOH$ to cleave the protective BOC group (Scheme 2). In the case of **87**, *N*-Z-6-aminocaproic acid was amidated with *N*-ethyl-*N*-(2-methoxy)-benzylamine[28] followed by the removal of the protecting group with catalytic hydrogenation over 10% palladium on charcoal (Scheme 3). The isopropyl derivative **90** was obtained by alkylation with acetone in reductive conditions of *N*-Z-1,6-diaminohexane, followed by the reaction of **88** with 2-methoxybenzyl chloride to give **89** and subsequent deprotection to the desired compound (Scheme 4).

The initial synthetic strategy to link the benzoquinone function to the diamines relied on the straightforward reaction between 1,4-benzoquinone and the appropriate diamine. In this way, the reaction between 1,4-benzoquinone and **69** gave **2** (Scheme 5).[23] Similarly, compounds **6** and **7** were obtained through the reaction of **69** with 2,5-dimethyl-1,4-benzoquinone and 2,5-diphenyl-1,4-benzoquinone, whereas **3**−**5** were obtained through the nucleophilic displacement of two halogen atoms respectively from 2,3,5,6-tetrafluoro-, 2,3,5,6-tetrachloro-, or 2,3,5,6-tetrabromo-1,4-benzoquinone by **69** (Scheme 5).

**Scheme 4.** Synthesis of Diamine **90**[a]

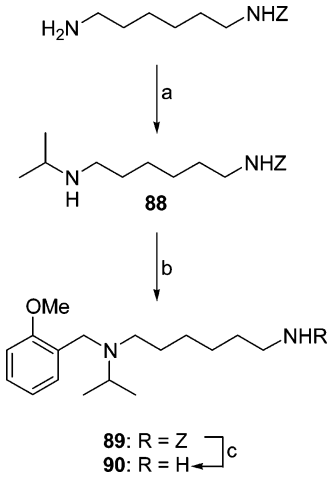


[a] Reagents and conditions: Z = $C_6H_5CH_2OCO-$; (a) MeCOMe, $NaBH_4$, EtOH, 60 °C, 48 h; (b) 2-$MeOC_6H_4CH_2Cl$, KI, $Et_3N$, DMF, 105 °C, 96 h; (c) 30% HBr, AcOH, 6 h.

**Scheme 5.** Synthesis of Quinone-Bearing Polyamines **2**−**7**[a]

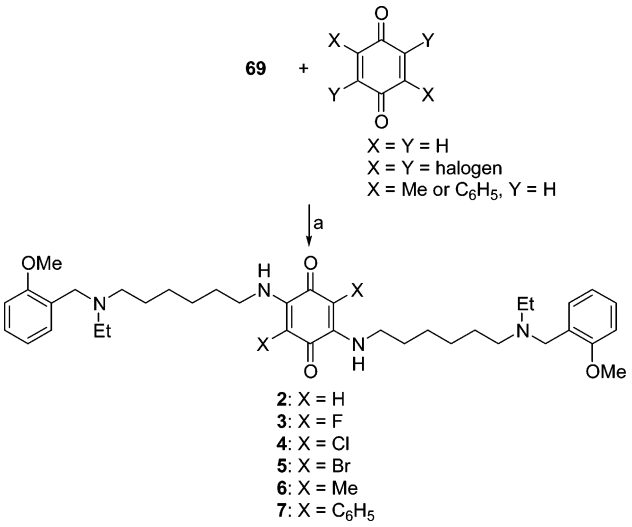


[a] Reagents and conditions: (a) for **2** see ref 21; for **3**−**5**, ether, rt, 1 h; for **6**, MeOH, rt, 20 h; for **7**, EtOH, 60 °C, 2 h.

However, the synthetic procedure for **2** afforded very complex mixtures, providing the desired 2,5-diaminoquinone in a yield not higher than 20%. Therefore, a more efficient reaction was developed, which involved substitution of the methoxy group of 2,5-dimethoxy-1,4-benzoquinone with an appropriate diamine (**65**−**83**). In this case, the yield increased to 60−100% and no chromatography purification was required for the synthesis of most of the final compounds (Scheme 6).

Finally, the aromatic analogue **8** was synthesized, starting from *N*-Z-6-aminocaproic acid and 1,4-phenylenediamine (Scheme 7). Treatment of **91** with HBr gave **92**, which was treated with 2-methoxybenzaldehyde and $NaBH_4$ to afford **93**, which, in turn, was ethylated (**94**) and finally reduced with borane to **8**.

## Biology

To determine their potential interest as MTDLs for the treatment of AD, **3**−**29** were assayed for their human AChE inhibitory activity. Furthermore, to establish the selectivity of **3**−**29**, their butyrylcholinesterase (BChE) inhibitory activity was also determined on BChE from human serum. The inhibitory

**Scheme 6.** Synthesis of Quinone-Bearing Polyamines **9**−**29**[a]

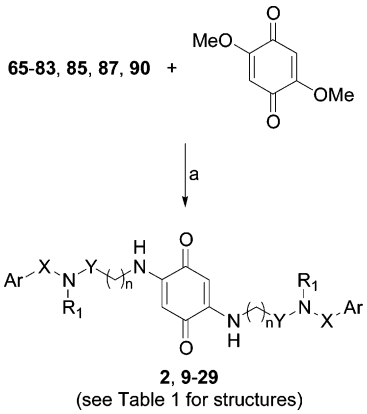


[a] Reagents and conditions: (a) EtOH, 60 °C, 5 h.

**Scheme 7.** Synthesis of the Aromatic Analogue **8**[a]

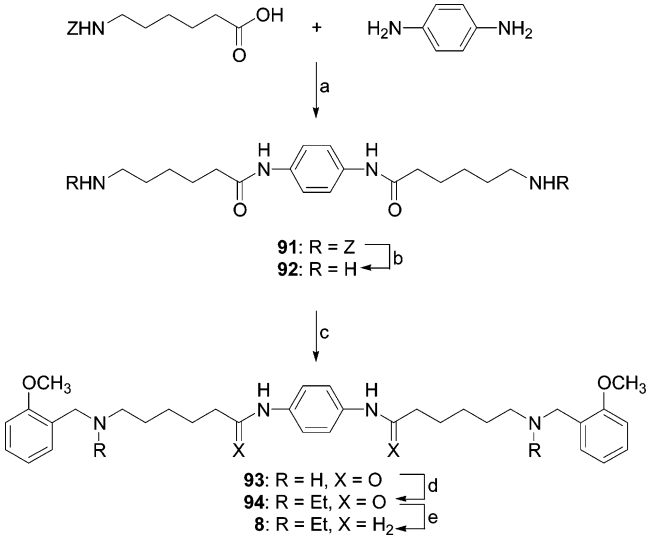


[a] Reagents and conditions: Z = $C_6H_5CH_2OCO-$; (a) EtOCOCl, $Et_3N$, dioxane, 12 h; (b) 30% HBr, AcOH/$CF_3COOH$, 4 h; (c) 2-$MeOC_6H_4CHO$, MeOH, reflux, 2 h, then $NaBH_4$, EtOH, rt, overnight; (d) diethyl sulfate, toluene, reflux, 6 h, then rt, overnight; (e) $BH_3$·MeSMe, diglyme, 120 °C, 8 h, MeOH, gaseous HCl.

potency is expressed as $IC_{50}$, which represents the concentration of inhibitor required to decrease the enzyme activity by 50% (Table 1).

The use of inhibitors of A$\beta$ oligomerization has emerged as a promising pharmacotherapy for AD. Therefore, the ability of selected quinone-bearing polyamines (**5**, **7**, **8**, **10**, **15**, **16**, and **24**) to inhibit the proaggregating action of AChE toward A$\beta$-(1−40) was assessed through a thioflavin T-based fluorometric assay (Table 1).[29,30] Not all the compounds were assayed to determine their ability to block AChE-mediated A$\beta$ aggregation, because this assay can be very expensive in light of the large quantities of enzyme and peptide needed for screening. The overall cost may be inaccessible for most of the academic laboratories.[31]

Compounds **1** and **3**−**29** were also tested in vitro to assess their potential to inhibit the self-induced aggregation of A$\beta$-(1−42).[32−34]

Different studies on the antioxidant properties of 1,4-benzoquinone derivatives, such as CoQ and idebenone, have conclusively demonstrated that the antioxidant activity pertains exclusively to their hydroquinone form, since the quinone, in principle, cannot scavenge radicals.[35] Furthermore, NAD(P)H: quinone oxidoreductase 1 (DT-diaphorase, NQO1; EC 1.6.99.2)

**Table 1.** Inhibition of AChE and BChE Activities and AChE-Mediated and Self-Induced A$\beta$ Aggregation by Quinone-Bearing Polyamines

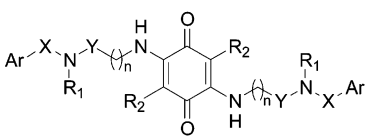

**2-7**, **9-29**

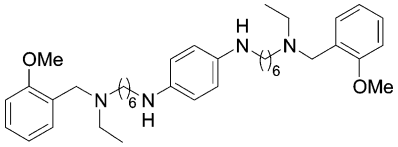

**8**

| compd no.[a] | Ar | X | $R_1$ | Y | *n* | $R_2$ | IC$_{50}$[b] (nM) AChE | IC$_{50}$[b] (nM) BChE | inhibition of A$\beta$ aggregation (%) AChE-induced[c] | inhibition of A$\beta$ aggregation (%) self-induced[d] |
|---|---|---|---|---|---|---|---|---|---|---|
| **1**[e] | | | | | | | 170 ± 2 | 11600 ± 300 | <5[f] | 20.3 ± 1.9 |
| **2** | 2-MeOC$_6$H$_4$ | $CH_2$ | Et | $CH_2$ | 5 | H | 1.55 ± 0.11[g] | 1440 ± 100[g] | 87.1 ± 1.7[g] | 66.8 ± 4.4 |
| **3** | 2-MeOC$_6$H$_4$ | $CH_2$ | Et | $CH_2$ | 5 | F | 5.17 ± 0.17 | 1520 ± 90 | nd[h] | 52.1 ± 11.7 |
| **4** | 2-MeOC$_6$H$_4$ | $CH_2$ | Et | $CH_2$ | 5 | Cl | 3.05 ± 0.29 | 800 ± 62 | nd | 68.2 ± 12.3 |
| **5** | 2-MeOC$_6$H$_4$ | $CH_2$ | Et | $CH_2$ | 5 | Br | 2.66 ± 0.19 | 696 ± 41 | 84.2 ± 2.5 | 63.9 ± 9.7 |
| **6** | 2-MeOC$_6$H$_4$ | $CH_2$ | Et | $CH_2$ | 5 | Me | 9.50 ± 0.23 | 462 ± 2 | nd | 68.0 ± 11.0 |
| **7** | 2-MeOC$_6$H$_4$ | $CH_2$ | Et | $CH_2$ | 5 | $C_6H_5$ | 123 ± 10 | 2250 ± 190 | 45.6 ± 0.8 | 68.2 ± 2.1 |
| **8** | | | | | | | 42.5 ± 1.9 | 505 ± 42 | 72.4 ± 2.0 | 56.5 ± 1.9 |
| **9** | 2-MeOC$_6$H$_4$ | $CH_2$ | Et | $CH_2$ | 1 | H | 61.5 ± 1.3 | 16800 ± 1100 | nd | 24.3 ± 3.8 |
| **10** | 2-MeOC$_6$H$_4$ | $CH_2$ | Et | $CH_2$ | 2 | H | 2.25 ± 0.21 | 9840 ± 340 | 91.1 ± 0.3 | 32.4 ± 4.7 |
| **11** | 2-MeOC$_6$H$_4$ | $CH_2$ | Et | $CH_2$ | 3 | H | 13.6 ± 0.5 | 12800 ± 800 | nd | 39.3 ± 1.8 |
| **12** | 2-MeOC$_6$H$_4$ | $CH_2$ | Et | $CH_2$ | 4 | H | 2.36 ± 0.13 | 3460 ± 180 | nd | 50.5 ± 2.1 |
| **13** | 2-MeOC$_6$H$_4$ | $CH_2$ | Et | $CH_2$ | 6 | H | 7.79 ± 0.37 | 1250 ± 250 | nd | 70.5 ± 0.5 |
| **14** | 2-MeOC$_6$H$_4$ | $(CH_2)_2$ | Et | $CH_2$ | 5 | H | 17.3 ± 1.4 | 518 ± 24 | nd | 71.4 ± 4.1 |
| **15** | 2-MeOC$_6$H$_4$ | $CH_2$ | Et | CO | 5 | H | 11600 ± 300 | 18500 ± 700 | <5 | 28.7 ± 10.2 |
| **16** | 2-MeOC$_6$H$_4$ | $CH_2$ | H | $CH_2$ | 5 | H | 123 ± 20 | 3230 ± 150 | 90.0 ± 5.4 | 69.9 ± 1.4 |
| **17** | 2-MeOC$_6$H$_4$ | $CH_2$ | Me | $CH_2$ | 5 | H | 77.8 ± 4.3 | 5110 ± 410 | nd | 70.4 ± 4.2 |
| **18** | 2-MeOC$_6$H$_4$ | $CH_2$ | iPr | $CH_2$ | 5 | H | 12.9 ± 0.6 | 660 ± 46 | nd | 58.5 ± 3.5 |
| **19** | $C_6H_5$ | $CH_2$ | Et | $CH_2$ | 5 | H | 73.3 ± 3.2 | 645 ± 33 | nd | 54.6 ± 1.7 |
| **20** | 4-MeOC$_6$H$_4$ | $CH_2$ | Et | $CH_2$ | 5 | H | 51.1 ± 1.0 | 2390 ± 110 | nd | 68.8 ± 1.3 |
| **21** | 3-MeOC$_6$H$_4$ | $CH_2$ | Et | $CH_2$ | 5 | H | 13.8 ± 1.7 | 1690 ± 60 | nd | 70.9 ± 1.4 |
| **22** | 2-MeC$_6$H$_4$ | $CH_2$ | Et | $CH_2$ | 5 | H | 71.9 ± 2.9 | 2080 ± 260 | nd | 46.9 ± 1.4 |
| **23** | 2-ClC$_6$H$_4$ | $CH_2$ | Et | $CH_2$ | 5 | H | 593 ± 51 | 45100 ± 1000 | nd | 22.7 ± 2.4 |
| **24** | 2-NO$_2$C$_6$H$_4$ | $CH_2$ | Et | $CH_2$ | 5 | H | 2310 ± 130 | 67100 ± 4000 | 34.6 ± 4.1 | 46.7 ± 1.3 |
| **25** | 2-furanyl | $CH_2$ | Et | $CH_2$ | 5 | H | 144 ± 3 | 3410 ± 200 | nd | 42.7 ± 1.4 |
| **26** | 2-thienyl | $CH_2$ | Et | $CH_2$ | 5 | H | 60.4 ± 4.1 | 2790 ± 220 | nd | 43.8 ± 0.2 |
| **27** | 2-pyridyl | $CH_2$ | Et | $CH_2$ | 5 | H | 125 ± 6 | 2470 ± 110 | nd | 21.5 ± 1.5 |
| **28** | 3-pyridyl | $CH_2$ | Et | $CH_2$ | 5 | H | 133 ± 6 | 11900 ± 700 | nd | 13.1 ± 5.6 |
| **29** | 4-pyridyl | $CH_2$ | Et | $CH_2$ | 5 | H | 192 ± 10 | 70100 ± 4700 | nd | 22.5 ± 1.5 |
| tacrine | | | | | | | 424 ± 21 | 45.8 ± 3.0 | 7[i] | <5 |
| donepezil | | | | | | | 23.1 ± 4.8 | 7420 ± 390 | 22[i] | <5 |
| galantamine | | | | | | | 2010 ± 150 | 20700 ± 1500 | 17.9 ± 0.1 | <5 |
| rivastigmine | | | | | | | 3030 ± 210 | 30.1 ± 14 | <5 | 17.8 ± 1.6 |
| propidium | | | | | | | 32300 | 13200 | 82.0 ± 2.5[i] | 61.1 ± 4.6 |
| Congo red | | | | | | | nd | nd | nd | 78.8 ± 0.9 |

[a] **1**, dihydrochloride; **2**−**29**, free bases. [b] Human recombinant AChE and BChE from human serum were used. IC$_{50}$ values represent the concentration of inhibitor required to decrease enzyme activity by 50% and are the mean of two independent measurements, each performed in triplicate. [c] Inhibition of AChE-induced A$\beta$(1−40). The concentration of the tested inhibitor and A$\beta$(1−40) was 100 $\mu$M and 230 $\mu$M, respectively, whereas the A$\beta$(1−40):AChE ratio was equal to 100:1. [d] Inhibition of self-induced A$\beta$(1−42) aggregation (50 $\mu$M) produced by the tested compound at 10 $\mu$M concentration. [e] See Figure 1 for structure. [f] Not significant. [g] Data from ref 21. [h] Not determined. [i] Data from ref 44.

**Table 2.** Ability of **2**, **5**, and **8** To Accept Electrons from the Enzyme NQO1

| compd no. | $K_m$ ($\mu$M) | $V_{max}$ [($\mu$mol/min)/mg] | compd no. | $K_m$ ($\mu$M) | $V_{max}$ [($\mu$mol/min)/mg] |
|---|---|---|---|---|---|
| **2** | 12.7 ± 1.3 | 3480 ± 20 | **8** | not active | |
| **5** | 15.1 ± 0.1 | 2588 ± 68 | menadione | 1.20 ± 0.05 | 7286 ± 55 |

was shown to play a role in the regeneration and maintenance of a CoQ-reduced antioxidant state. This inducible enzyme catalyzes the two-electron reduction of quinones to hydroquinones, bypassing the production of semiquinones and, consequently, preventing their participation in redox-cycling and the subsequent generation of reactive oxygen species (ROS).[35] Thus, compounds **2**, **5**, and **8** were tested with respect to their ability to accept electrons from NAD(P)H via NQO1, in comparison with menadione as a reference compound, by following the absorbance change of NADH. The results are expressed in terms of the apparent $V_{max}$ and $K_m$ (Table 2).

**Table 3.** Effects of **2**, **5**, and **8** on ROS Formation in SH-SY5Y Cells[a,b]

| concn ($\mu$M) | intracellular ROS increase, % 2 | 5 | 8 |
|---|---|---|---|
| 0 | 53.00 ± 6.55 | 53.00 ± 6.55 | 53.00 ± 6.55 |
| 0.1 | 52.67 ± 4.07 | 50.51 ± 4.05 | 54.20 ± 5.45 |
| 0.3 | 49.94 ± 6.12 | 52.35 ± 3.22 | 50.45 ± 4.50 |
| 1.0 | 40.25 ± 8.45[c] | 50.43 ± 4.35 | 51.35 ± 6.50 |
| 3.0 | 30.50 ± 4.30[d] | 42.12 ± 4.45[c] | 49.54 ± 3.55 |

[a] The experiments were performed with human neuronal-like cells (SH-SY5Y) expressing high levels of NQO1. [b] The results are expressed as the percentage increase of intracellular ROS evoked by exposure to *t*-BuOOH. The values are reported as the mean ± SD of three independent experiments (treated vs untreated). [c] $p < 0.01$. [d] $p < 0.001$ at ANOVA with the Scheffe post hoc test.

The antioxidant activity of **5** and **8** was also evaluated against formation of ROS in human neuronal-like cells (SH-SY5Y) after treatment with *t*-BuOOH, a compound used to induce oxidative damage.[36] Experiments were performed with SH-SY5Y cells

treated with sulforaphane, a phase 2 enzyme inducer, to overexpress cytosolic NQO1 (Table 3).[37]

In all the assays, **2** was used as a reference compound.

### Docking, Cluster Analysis, and Molecular Dynamics Simulations

Docking simulations were carried out using the GOLD v3.0.1 package of software.[38] Compounds **2**, **7**, **8**, and **10** were docked at the gorge of the human AChE (PDB code 1B41).[39] The docking outcomes were rationalized using the software AClAP v1.0.[40,41] The binary complex between **2** and AChE was further investigated by means of molecular dynamics (MD) simulations in the nanosecond time scale carried out with the AMBER 8.0 package of software.[42]

### Results and Discussion

Recently, we reported that polyamines related to **1** could represent a valuable lead for the design of compounds useful for investigating AD because of (i) their improvement of cholinergic transmission by inhibiting the catalytic site of AChE and (ii) their interaction with the AChE peripheral anionic site (PAS), which might prevent AChE-mediated A$\beta$ aggregation.[17,22,43]

To obtain MTDLs useful for AD therapy, we inserted into the polyamine backbone of **1** a 1,4-benzoquinone moiety that could confer to the resulting molecules additional properties beneficial in the treatment of AD. The significant effectiveness of **2** in reverting neurodegeneration in vivo[23] strongly supported the feasibility of the MTDL approach to the treatment of AD. It formed the basis for the development of a new class of small-molecule-based MTDLs that can serve as powerful tools both in understanding the role and function of the multiple emerging biological targets and in further validating the design rationale.

A major concern regarding SAR studies of MTDLs is that there is no a priori selection for small molecules to be synthesized over others, because the properties of the selected molecular targets usually differ. Nevertheless, it is worth noting that, of the four selected targets, i.e., (a) cholinesterases (AChE and BChE), (b) A$\beta$ aggregation induced by human AChE, (c) self-induced A$\beta$ aggregation, and (d) oxidative stress, the first two are supposedly related since AChEI binding at PAS may interfere with AChE proaggregating action.[29,30] Therefore, some selection might be based on the inhibitor mechanism of action and docking studies.

We circumvented the general lack of uniform structural information by synthesizing a small unbiased library of derivatives of **2**, trying to analyze the contributions of the different structural elements of the molecule to the different activities.

Starting from **2**, the 2,3,5,6-tetrasubstituted 1,4-benzoquinones **3**−**7** were the first quinone-bearing polyamines to be synthesized. Compound **8** was included in the present study because its phenyl ring is planar, like the 1,4-benzoquinone moiety, and can give information on the importance of the quinone functionality on the biological profile of this new series of MTDLs. The role of the distance between the inner and the outer nitrogen atoms and between the outer nitrogen atoms and the terminal phenyl ring was studied by synthesizing the analogues **9**−**13** and **14**, in which the hexamethylene chain and the methylene group were respectively replaced by a spacer composed of two to seven methylene units or by two methylenes. Next, the importance of the terminal amine function of **2** on the biological profile was evaluated by synthesizing the amide analogue **15**. Since, in a previous study,[43] we verified that, in polyamines related to **1**, AChE inhibition was significantly dependent on the type of substituent on the benzylic nitrogen atoms, we included in this study compounds **16**−**18**, in which the *N*-ethyl group was replaced by a hydrogen atom, a methyl group, or an isopropyl group. Furthermore, notwithstanding that a 2-methoxybenzyl group seems to play a crucial role in the affinity toward AChE as revealed by **1** analogues,[20,32] we decided to further investigate the role of different aromatic substituents (**19**−**29**) in the hope of acquiring further information about the structural requirements for targeting the biological counterparts, other than AChE, investigated in the present study.

**AChE Inhibition**. The inhibitory potency of compounds **3**−**29** on human recombinant AChE and BChE from human serum was assessed through comparison with the prototypic polyamines **1** and **2**, the AChEIs donepezil, galantamine, rivastigmine, and tacrine, marketed for the treatment of AD, and propidium, a specific inhibitor of the AChE PAS (Table 1).

All the compounds **2**−**29** showed AChE inhibition activity with $IC_{50}$ values ranging from 1.55 to 11600 nM while displaying a much lower affinity for BChE. These results are particularly intriguing because, contrary to a previous view,[44] BChE may have a role inverse to that of AChE in AD.[45] Thus, selectivity for AChE over BChE may be beneficial for AD treatment. An analysis of the results reported in Table 1 reveals that AChE, but not BChE, inhibition can be markedly affected by the introduction of substituents on the benzoquinone moiety. It turned out that the halogen-bearing analogues **3**−**5** were only slightly less potent (2−3-fold) than **2**, whereas **6** and **7** displayed a significantly lower affinity toward AChE, being from 6- to 79-fold less potent. Interestingly, the replacement of the benzoquinone moiety of **2** with a phenyl ring, as in **8**, reduced the inhibition of AChE 27-fold, revealing that the two oxygen atoms of **2** may have, in addition to the other properties outlined below, a role in the interaction process with the enzyme.

The discovery that **10** and **12** (but not **9**, **11**, and **13**), which are endowed with a shorter distance between the inner and the outer nitrogen atoms, showed an affinity for AChE that is only slightly lower than that of **2** may indicate that the hexamethylene spacer of **2** interacts with the enzyme with a (partially) folded conformation. Interestingly, all the compounds with a shorter distance (**9**−**12**) were weaker BChE inhibitors than **2**. Lengthening the distance between the outer nitrogen atoms and the phenyl rings, as in **14**, caused a significant decrease in the affinity for AChE relative to that of **2**, suggesting that the terminal benzyl moieties are endowed with optimal properties for interaction with the enzyme. The importance of the nature of the terminal nitrogen atoms of **2** in the interaction with AChE was evaluated by investigating compounds **15**−**18**. The dramatic decrease in affinity toward AChE observed for the amide analogue **15** indicated that the terminal nitrogen atoms of this series of quinone-bearing polyamines must be basic. In agreement with previous results obtained with polyamines related to **1**,[43] compounds **16**−**18**, bearing a hydrogen atom, a methyl group, or an isopropyl group, respectively, inhibited AChE activity with a lower affinity than that shown by **2**, which bears an ethyl group on the terminal nitrogen atoms. Finally, the results observed for **19**−**29** clearly suggest that a 2-methoxybenzyl group on the terminal nitrogen atoms may be endowed with the optimal electronic and lipophilic properties for interaction with AChE (Table 1).

**Computational Studies of the AChEI Binding Mode**. To investigate the binding mode of **2** and some of its derivatives at the human AChE gorge, docking simulations and cluster analyses were carried out. In addition, the binary complex

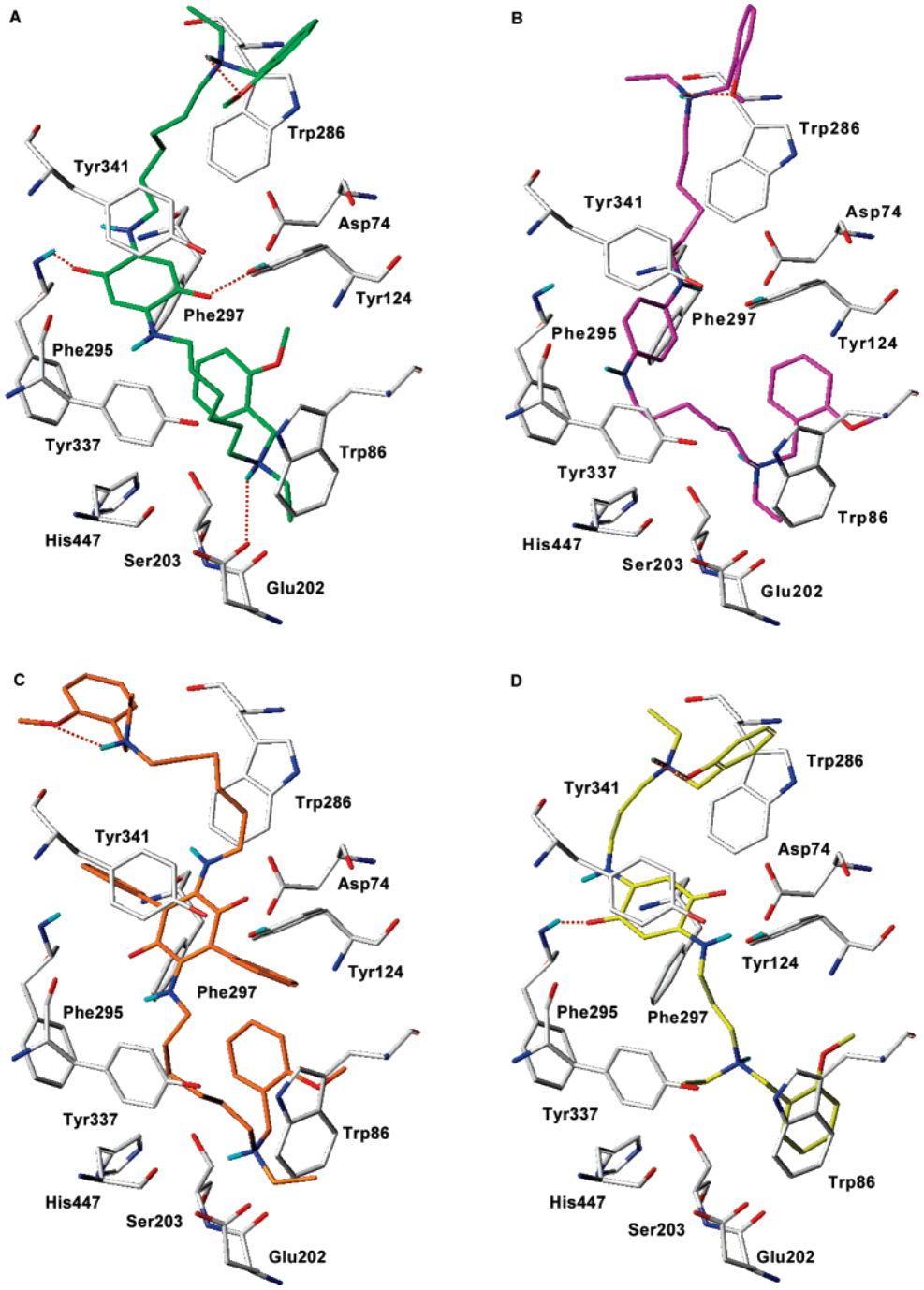


**Figure 2.** Binding mode of some AChEIs as outcomes of docking simulations. H-bonds are dark-red dotted lines. Notably, an intramolecular H-bond was always identified between one protonated nitrogen and one *o*-methoxyphenyl ring. (A) Binding mode of **2** (carbon atoms in green) at the hAChE gorge. The conformation was selected within a stable MD simulation interval between 2 and 5 ns. The quinone moiety is able to tightly anchor the molecule by means of H-bonds. (B) Binding mode of **8** (carbon atoms in magenta) at the hAChE gorge. The benzene ring can hydrophobically interact with some aromatic residues (Tyr124 and Tyr341); however, these interactions are probably less tight than those observed in the binding mode of **2**. (C) Binding mode of **7** (carbon atoms in orange) at the hAChE gorge. The phenyl rings in positions 3 and 6 of the quinone prevent the formation of the H-bonds that we could observe in the binding mode of **2**. Moreover, one phenyl ring, pointing toward Asp74, is probably responsible for an electrostatic repulsion between the $\pi$-system of **7** and the carboxylate group of the aspartic acid. (D) Binding mode of **10** (carbon atoms in yellow) at the hAChE gorge. The aliphatic chain of three methylenes was long enough for a proper interaction between our derivatives and both the Trp286 and Trp86 sites. The quinone moiety can establish H-bond interactions with residues located at the hAChE midgorge.

between **2** and AChE was then submitted to 7 ns of MD simulations. The conformation of **2** reported in Figure 2A was selected within a stable simulation interval (2−5 ns), and it clearly shows that the benzylammonium ends of **2** were able to contact Trp86 and Trp286 belonging to the catalytic and peripheral sites of the enzyme, respectively. Both interactions were quite stable during the MD simulations. This dynamic behavior was quite different from that observed for the prototypic polyamine **1**, which turned out to be dynamically less stable during a few nanoseconds of MD simulations.[17] In this case, because of the highly flexible chain linking its benzylammonium moieties, we could not definitively conclude that **1** was able to tightly interact with both sites of the AChE enzyme.[17] Notwithstanding that **1** and **2** were able to simultaneously contact both sites of AChE, only extensive MD simulations could give meaningful information about their markedly dif-

ferent AChE inhibitory profiles, providing a possible explanation for the relatively low potency of **1**. A pivotal role for the different dynamical behavior of **2** when compared to **1** may be related to the benzoquinone moiety, which could establish favorable interactions with amino acids of the enzyme midgorge.[46] Indeed, the carbonyl oxygen atoms can establish H-bonds either with −OH of tyrosine side chains (Tyr341 and Tyr124)[23] or with −NH of the Phe295 backbone (Figure 2A). One can therefore conclude that the benzoquinone moiety of **2** is fundamental for properly anchoring the molecule at the enzyme gorge, thus allowing it to tightly interact with both the catalytic and peripheral anionic sites of the enzyme. This structural feature could be responsible for the experimentally observed capability of **2** to inhibit the AChE-induced A$\beta$ aggregation (see below).

To investigate more deeply the role of the benzoquinone moiety in the inhibition of the AChE-induced A$\beta$ aggregation, docking simulations were also performed with **8**, a compound in which the benzoquinone moiety of **2** was substituted with a phenyl ring. Notably, **8** was able to inhibit AChE-induced A$\beta$ aggregation to a lesser extent when compared to **2**. However, **8** was a more potent AChEI than **1**. Docking simulations (Figure 2B) clearly show that the central phenyl ring is responsible for anchoring the molecule at the AChE gorge, by means of hydrophobic and $\pi-\pi$ stacking interactions. Obviously, the tight H-bond network of the benzoquinone of **2** was not observed for the phenyl ring of **8**, which probably explains the slightly lower inhibitory potency of **8** relative to **2** toward the AChE-induced A$\beta$ aggregation.

Docking simulations were also carried out with **7** and **10**. For **7** (Figure 2C), we could observe a detrimental role for two phenyl rings in positions 3 and 6 of the benzoquinone ring. In fact, such bulky substituents prevented a proper orientation of **7** within the gorge, which probably accounts for its reduced inhibitory potencies, when compared to those of **2** (Table 1), toward both AChE catalytic activity and AChE-induced A$\beta$ aggregation. Conversely, docking simulations carried out with **10** (Figure 2D) clearly showed that an aliphatic chain of three methylenes was long enough for an optimal inhibition profile toward both AChE and AChE-induced A$\beta$ aggregation, as is clearly demonstrated by its biological profile, reported in Table 1.

Finally, MD simulations carried out on the binary complex AChE−**2** could also explain the 3 orders of magnitude difference between AChE and BChE inhibitory potencies. Since the latter enzyme lacks PAS, BChE cannot interact with **2** as tightly as AChE does.

**Inhibition of A$\beta$ Aggregation**. We have already demonstrated that polyamines and quinone-bearing polyamines, exemplified by **1** and **2**, respectively, cause a mixed-type inhibition of AChE, that is, inhibition of both the catalytic site and PAS of the enzyme.[22] The availability of a suitable test for the determination of the A$\beta$(1−40) aggregation mediated by AChE allowed us to verify whether such "dual acting" [47] AChEIs are able to decrease or block AChE-induced A$\beta$ aggregation. In view of the high cost of the test, we selected a narrow number of compounds to investigate some key aspects, namely, the optimum spacer chain length (**2** vs **10**), the importance, if any, of the benzoquinone fragment (**2** vs **8**) and of its substituents (**5** and **7**), and the basicity of the terminal nitrogen atoms (**2** vs **16** and **24** and **2** vs the amide analogue **15**). The results were compared with those of prototypes **1** and **2** and AChEIs tacrine, donepezil, galantamine, rivastigmine, and propidium[48] (Table 1). Of the reference compounds, **1**, tacrine, donepezil, galantamine, and rivastigmine were not able to inhibit to a significant extent AChE-induced A$\beta$ aggregation, whereas propidium blocked the aggregation process by 82.0 ± 2.5%. Quinone-bearing polyamines **2**, **5**, **10**, and **16** at the same concentration inhibited almost completely AChE-induced A$\beta$ aggregation. The amide analogue **15** was devoid of activity, whereas **7**, **8**, and **24** significantly blocked, although to a lesser extent than **2**, A$\beta$ aggregation mediated by AChE. These results clearly suggest that a basic nitrogen atom is essential for inhibiting A$\beta$ aggregation (compare **15** to **2**), whereas a substituent on the benzoquinone moiety may not favor the A$\beta$ aggregation inhibition process. Furthermore, the high antiaggregating activity displayed by **16** and **8**, despite their lower AChE inhibitory potency, appears to validate our previous hypothesis that the ability to simultaneously bind both the catalytic site and PAS of AChE is not a sufficient condition for strongly inhibiting A$\beta$ aggregation mediated by the enzyme. In addition, a comparison of **2** to **8** reveals that the benzoquinone moiety, while important, may not be essential for inhibiting AChE-induced A$\beta$ aggregation.

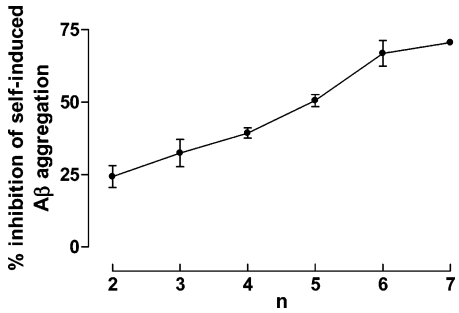


**Figure 3.** Effect of the chain length *n* between the inner and outer nitrogen atoms [$N(CH_2)_nN$] of **2** and **9**−**13** on the inhibition of the self-induced A$\beta$(1−42) aggregation.

Besides assessing the ability to inhibit AChE-induced A$\beta$-(1−40) aggregation, which is likely to be relevant in the brain of AD patients,[49] we tested all the compounds (inhibitor:A$\beta$ ratio 1:5) to assess the structural elements responsible for the in vitro inhibition of the self-assembly of A$\beta$(1−42), which is the most amyloidogenic A$\beta$ fragment found in the AD plaques.

The near-identical inhibition percentage provided by tetra-substituted quinones **3**−**7** with respect to **2** points to the conclusion that the presence of additional substituents on the quinone core is irrelevant against the self-induced A$\beta$ aggregation. Conversely, a major role seems to be played by the length of the spacer, since the potency was increased by increasing the length between the inner and outer nitrogen atoms from two to six methylene units as graphically shown in Figure 3. Interestingly, the potency remained almost unchanged on going from six (**2**) to seven (**13**) methylenes. The conclusion that six/seven methylenes may represent the optimal spacer length was further confirmed by the observation that **14** was as potent as **2** and **13**, which clearly suggests that the global length between the benzoquinone moiety and the terminal phenyl rings may be influential on the inhibition of the self-mediated A$\beta$ aggregation.

Furthermore, the type of the terminal nitrogen atom also seems relevant, since the amide derivative **15** was significantly less potent than **2**. In addition, the amine derivatives **16**−**18** were as potent as **2**, whereas the *N*-*i*-Pr derivative **18** resulted in a weaker inhibitor, owing to a possible steric hindrance of the *i*-Pr over H/Me/Et groups. The results observed for **15**−**18** may allow us to hypothesize that the fibril-binding properties of **2** are probably due to the presence of a symmetrical protonated structure, with charges spaced across a hydrophobic scaffold, which is also typical of classical azo-dye inhibitors of amyloid aggregation, such as Congo red.[50]

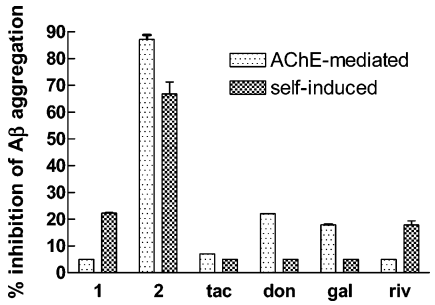


**Figure 4.** Inhibition of A$\beta$ aggregation. When the AChE-mediated aggregation was measured, the concentration of inhibitor and A$\beta$(1−40) was 100 and 230 $\mu$M, respectively, whereas the A$\beta$(1−40):AChE ratio was equal to 100:1. The inhibition of the self-induced A$\beta$(1−42) aggregation (50 $\mu$M) was produced by the tested compound at a 10 $\mu$M concentration.

The main conclusions regarding the compounds modified in the terminal aromatic moieties are that the methoxy derivatives **20** and **21** were as active as, if not slightly more potent than, **2** in inhibiting A$\beta$ aggregation (it is worth noting that, unlike AChE inhibitory potency, this potency was not influenced by the position of the methoxy group). It is also clear that replacing the phenyl moiety of **2** with different heteroaromatic rings resulted in weaker inhibitors of the self-induced A$\beta$ aggregation (compare **25**−**29** to **2**).

As shown in Figure 4, a comparison of the A$\beta$ antiaggregating properties of **2** to those of the four marketed AChEIs (tacrine, donepezil, galantamine, and rivastigmine) highlights the much better profile of **2** as far as both AChE- and self-induced A$\beta$ aggregation inhibition are concerned.

**Antioxidant Activity**. The antioxidant properties of **2**, **5**, and **8** were first verified by testing their ability to accept electrons from NAD(P)H via NQO1 (Table 2). As one would expect, it turned out that **2** and **5**, but not **8**, are good substrates for NQO1, being not very different from menadione in terms of reduction by the enzyme. To further confirm the NQO1-mediated mechanism of action, we showed that **2**, **5**, and menadione activities were sensitive to the NQO1 competitive inhibitor dicoumarol. In this situation, and parallel to its function in maintaining CoQ in its reduced antioxidant state, NQO1 may extend the antioxidant potential of this class of quinone derivatives through the generation of the corresponding hydroquinones, which have been suggested to have superior antioxidant properties.[51] Furthermore, the two-electron reduction of quinones by NQO1 should bypass semiquinone production, preventing the generation of ROS that would form by the interaction of the semiquinone with oxygen. More interestingly, an increase in NQO1 activity and localized changes have been shown in brain tissue from AD patients as compared to controls, suggesting an NQO1 up-regulation in response to the oxidative stress of the AD process.[52] Quinone-bearing compounds **2** and **5**, being specifically reduced by NQO1 into the corresponding hydroquinones, may exert their antioxidant activity in those brain regions affected by AD, where a close relationship exists between NQO1 activity and AD pathology.

The antioxidant studies were extended to a cell-based system, SH-SY5Y cells, in the presence or absence of an NQO1 inducer, such as sulforaphane.

The intracellular antioxidant activity of **2**, **5**, and **8** against the formation of ROS was assessed by using a range of concentrations of tested compounds that did not affect neuronal viability (0.1−3 $\mu$M). As shown in Table 3, SH-SY5Y cells expressing high levels of NQO1 treated with **2** showed a significant dose-dependent inhibitory effect on the ROS formation at a concentration of 1 $\mu$M ($p < 0.01$) and 3 $\mu$M ($p < 0.001$), while treatment with **5** produced a significant decrease of ROS formation only with the highest concentration used (3 $\mu$M). In contrast, when treated with **8**, the neuronal cells did not show any difference on ROS formation. Taken together, these results show that, via NQO1, compounds **2** and **5** (but not **8**) are able to protect neuronal cells against ROS formation evoked by oxidative stress, with compound **2** being the most active.

**MTDLs for AD Treatment**. The results of our efforts to obtain new MTDLs endowed with an in vitro profile appropriate for identifying novel lead candidates for a disease-modifying treatment of AD show how, in the MTDL context, structural variations can lead to different biological outcomes depending on the target investigated. This highlights the difficulty of designing proper analogue series targeted at several systems simultaneously. Compounds **2**, **5**, and **8** are representative of some modifications that we introduced into the polyamine skeleton of **1** with the aim of "fine-tuning" the ligand's structure toward a suitable MTDL lead candidate. As stated above, given the lack of a uniform structural guidance for the design of new molecules, the adopted strategy involved the initial synthesis of a small library of varied compounds followed by testing in a first assay system (AChE/BChE inhibition) and then the sequential exploration of other biological activities on the "most interesting" compounds. Indeed, the parallel screening of all the activities would have provided a complete set of results, but we reasoned that, if the first test addressed an action deemed crucial in the pathological context (in our case, AChE inhibition), it was reasonable to take a more conservative and economic approach by selecting only the best performers for subsequent steps of biological testing.

By examining the results of the present investigation, a kind of "multivariate" SAR of the polyamine−quinones emerge, showing how we can vary the biological profiles by changing selected structural elements of the molecules. The resulting information is the identification of the set of moieties that provides the best overall action against the target biological systems, leading to the optimization of the starting compounds. In this regard, the data obtained confirm that **2** was indeed the best molecule for addressing the different biological end points relevant in the AD pathology.

As a general comment, the relevance of the results obtained in in vitro models may suffer from the major drawback represented by the different concentrations at which an MTDL hits different targets. In this respect, only proof-of-concept by means of in vivo experiments can provide a definite answer to this issue, which, in our opinion, is the most relevant in the development of efficacious MTDLs.

## Conclusions

Nowadays the drug discovery approach is changing, because the "one-molecule, one-target" paradigm cannot provide the right answer to all the quests for new medicines, due to the fact that many pathologies are multifactorial in nature. Hence, a single drug, despite a high specificity for a given target, might be devoid of practical utility for the treatment of complex syndromes such as neurodegenerative diseases. It is emerging that these latter disorders can be better approached with a drug design strategy leading to MTDLs. Here, a critical feature of the approach, i.e., the possibility of using small molecules to target different functions of the AD pathogenic pathway, is clearly demonstrated.

## Experimental Section

Melting points were taken in glass capillary tubes on a Buchi SMP-20 apparatus and are uncorrected. IR and direct infusion ESI-MS spectra were recorded on Perkin-Elmer 297 and Waters ZQ 4000 apparatuses, respectively. $^1$H NMR spectra were recorded on Varian VXR 200 and 300 instruments. Chemical shifts are reported in parts per millions (ppm) relative to the peak for tetramethylsilane (TMS), and spin multiplicities are given as s (singlet), br s (broad singlet), d (doublet), t (triplet), br t (broad triplet), q (quartet), sept (septet), or m (multiplet). Although IR spectral data are not included (because of the lack of unusual features), they were obtained for all compounds reported, and they were consistent with the assigned structures. The elemental compositions of the compounds agreed to within ±0.4% of the calculated value. Where the elemental analysis is not included, crude compounds were used in the next step without further purification. Chromatographic separations were performed on silica gel columns by flash (Kieselgel 40, 0.040−0.063 mm, Merck) or gravity (Kieselgel 60, 0.063−0.200 mm, Merck) column chromatography. Reactions were followed by thin-layer chromatography (TLC) on Merck (0.25 mm) glass-packed precoated silica gel plates (60 F254) and then visualized in an iodine chamber or with a UV lamp. The term "dried" refers to the use of anhydrous sodium sulfate. Compounds were named following IUPAC rules as applied by Beilstein-Institute AutoNom (version 2.1), a PC-integrated software package for systematic names in organic chemistry.

**General Procedure for the Synthesis of 30−46**. A solution of the appropriate carbamic acid benzyl ester[53] and the corresponding substituted aldehyde in a 1:1.2 molar ratio in toluene was stirred at the refluxing temperature in a Dean−Stark apparatus for 6 h. After cooling, the solvent was evaporated, and the residue was dissolved in EtOH, cooled in an ice bath, and treated with $NaBH_4$ (1.2 equiv). The reaction mixture was stirred overnight at room temperature and then made acidic with 3 N HCl. The solution was concentrated, and the residue was taken up with $H_2O$ and washed with ether. The aqueous phase was made basic with 40% NaOH and extracted with $CHCl_3$. Removal of the dried solvents afforded the desired compound.

**[2-(2-Methoxybenzylamino)ethyl]carbamic Acid Benzyl Ester (30)**. **30** was synthesized from (2-aminoethyl)carbamic acid benzyl ester and 2-methoxybenzaldehyde: yellow oil; 80% yield.

**[3-(2-Methoxybenzylamino)propyl]carbamic Acid Benzyl Ester (31)**. **31** was synthesized from (3-aminopropyl)carbamic acid benzyl ester and 2-methoxybenzaldehyde: colorless oil; 90% yield.

**[4-(2-Methoxybenzylamino)butyl]carbamic Acid Benzyl Ester (32)**. **32** was synthesized from (4-aminobutyl)carbamic acid benzyl ester and 2-methoxybenzaldehyde: colorless oil; quantitative yield.

**[5-(2-Methoxybenzylamino)pentyl]carbamic Acid Benzyl Ester (33)**. **33** was synthesized from (5-aminopentyl)carbamic acid benzyl ester and 2-methoxybenzaldehyde: colorless oil; 92% yield.

**[6-(2-Methoxybenzylamino)hexyl]carbamic Acid Benzyl Ester (34)**. **34** was synthesized as previously described.[23]

**[7-(2-Methoxybenzylamino)heptyl]carbamic Acid Benzyl Ester (35)**. **35** was synthesized from (7-aminoheptyl)carbamic acid benzyl ester and 2-methoxybenzaldehyde: pale yellow oil; 90% yield.

**[6-(2-Methylbenzylamino)hexyl]carbamic Acid Benzyl Ester (36)**. **36** was synthesized from (6-aminohexyl)carbamic acid benzyl ester and 2-methylbenzaldehyde: yellow oil; 55% yield.

**[6-(2-Chlorobenzylamino)hexyl]carbamic Acid Benzyl Ester (37)**. **37** was synthesized from (6-aminohexyl)carbamic acid benzyl ester and 2-chlorobenzaldehyde: pale yellow oil; 65% yield.

**[6-(2-Nitrobenzylamino)hexyl]carbamic Acid Benzyl Ester (38)**. **38** was synthesized from (6-aminohexyl)carbamic acid benzyl ester and 2-nitrobenzaldehyde: yellow oil; 95% yield.

**(6-Benzylaminohexyl)carbamic Acid Benzyl Ester (39)**. **39** was synthesized from (6-aminohexyl)carbamic acid benzyl ester and benzaldehyde: colorless oil; quantitative yield.

**[6-(4-Methoxybenzylamino)hexyl]carbamic Acid Benzyl Ester (40)**. **40** was synthesized from (6-aminohexyl)carbamic acid benzyl ester and 4-methoxybenzaldehyde: pale yellow oil; 78% yield.

**[6-(3-Methoxybenzylamino)hexyl]carbamic Acid Benzyl Ester (41)**. **41** was synthesized from (6-aminohexyl)carbamic acid benzyl ester and 3-methoxybenzaldehyde: pale yellow oil; 76% yield.

{**6-[(Furan-2-ylmethyl)amino]hexyl**}**carbamic Acid Benzyl Ester (42)**. **42** was synthesized from (6-aminohexyl)carbamic acid benzyl ester and furan-2-carboxaldehyde: brown solid; mp 132−135 °C; 72% yield.

{**6-[(Thiophen-2-ylmethyl)amino]hexyl**}**carbamic Acid Benzyl Ester (43)**. **43** was synthesized from (6-aminohexyl)carbamic acid benzyl ester and thiophene-2-carboxaldehyde: yellow oil; 90% yield.

{**6-[(Pyridin-2-ylmethyl)amino]hexyl**}**carbamic Acid Benzyl Ester (44)**. **44** was synthesized from (6-aminohexyl)carbamic acid benzyl ester and pyridine-2-carboxaldehyde: yellow oil; 55% yield.

{**6-[(Pyridin-3-ylmethyl)amino]hexyl**}**carbamic Acid Benzyl Ester (45)**. **45** was synthesized from (6-aminohexyl)carbamic acid benzyl ester and pyridine-3-carboxaldehyde: yellow oil; 50% yield.

{**6-[(Pyridin-4-ylmethyl)amino]hexyl**}**carbamic Acid Benzyl Ester (46)**. **46** was synthesized from (6-aminohexyl)carbamic acid benzyl ester and pyridine-4-carboxaldehyde: yellow oil; 60% yield.

**General Procedure for the Synthesis of 47−50 and 52−55**. A mixture of compounds **30**−**33** or **35**−**38** and diethyl sulfate in toluene (1:2 molar ratio) was refluxed for 6 h and then stirred overnight at room temperature. After removal of toluene, the residue was washed several times with petroleum ether. The crude material was then dissolved in $H_2O$, made basic with 2 N NaOH, and extracted with $CHCl_3$. The dried organic phases were evaporated to afford an oil that was purified by flash chromatography.

{**2-[Ethyl(2-methoxybenzyl)amino]ethyl**}**carbamic Acid Benzyl Ester (47)**. **47** was obtained from **30**: eluent $CHCl_3$/toluene/MeOH/aqueous 28% ammonia (8:2:0.3:0.02); yellow oil; 45% yield.

{**3-[Ethyl(2-methoxybenzyl)amino]propyl**}**carbamic Acid Benzyl Ester (48)**. **48** was obtained from **31**: eluent petroleum ether/$CH_2Cl_2$/MeOH/aqueous 28% ammonia (5.0:4.6:0.4:0.04); colorless oil; 70% yield.

{**4-[Ethyl(2-methoxybenzyl)amino]butyl**}**carbamic Acid Benzyl Ester (49)**. **49** was obtained from **32**: eluent $CH_2Cl_2$/petroleum ether/EtOH/aqueous 28% ammonia (7:2.5:0.5:0.04); yellow oil; 51% yield.

{**5-[Ethyl(2-methoxybenzyl)amino]pentyl**}**carbamic Acid Benzyl Ester (50)**. **50** was obtained from **33**: eluent $CH_2Cl_2$/MeOH (9.25:0.75); yellow oil; 60% yield.

{**7-[Ethyl(2-methoxybenzyl)amino]heptyl**}**carbamic Acid Benzyl Ester (52)**. **52** was obtained from **35**: eluent $CHCl_3$/petroleum ether/MeOH/aqueous 28% ammonia (8:2:0.5:0.02); yellow oil; 35% yield.

{**6-[Ethyl(2-methylbenzyl)amino]hexyl**}**carbamic Acid Benzyl Ester (53)**. **53** was obtained from **36**: eluent $CH_2Cl_2$/petroleum ether/MeOH/aqueous 28% ammonia (8:2:0.3:0.015); yellow oil; 40% yield.

{**6-[(2-Chlorobenzyl)ethylamino]hexyl**}**carbamic Acid Benzyl Ester (54)**. **54** was obtained from **37**: eluent petroleum ether/$CH_2Cl_2$/MeOH (7:2.5:0.5); colorless oil; 40% yield.

{**6-[Ethyl(2-nitrobenzyl)amino]hexyl**}**carbamic Acid Benzyl Ester (55)**. **55** was obtained from **38**: eluent petroleum ether/$CHCl_3$/MeOH/aqueous 28% ammonia (8:2:0.4:0.02); green oil; 40% yield.

{**6-[Ethyl(2-methoxybenzyl)amino]hexyl**}**carbamic Acid Benzyl Ester (51)**. Acetaldehyde (29 mL, 0.51 mol) was added to a solution of KOH (4.2 g, 0.07 mol) and **34**[23] (hydrochloride salt; 104 g, 0.26 mol) in methanol (1.2 L) in a three-necked flask equipped with a mechanical stirrer. After the resulting solution was stirred at room temperature for 15 min, a solution of $NaBH_3CN$ (6.3 g, 0.1 mol) in methanol (50 mL) was added dropwise, and the resulting mixture was stirred overnight. Then KOH (15 g) was added, and the obtained suspension was suction-filtered through Celite and concentrated under vacuum at a temperature lower than 45 °C. A solid was obtained, which was partitioned between water and $CH_2Cl_2$ (2 × 750 mL). The combined organic extracts were

dried and evaporated to give the raw product (106 g), which was purified by flash chromatography. Eluting first with $CHCl_3$ and then with $CHCl_3$/EtOH (9.3:0.7) provided pure **51** in 48% yield. Alternatively, the raw product could be purified by multiple extractions with hot petroleum ether. The combined and dried extracts gave **51** in 53% yield, which was sufficiently pure for most purposes.

**General Procedure for the Synthesis of 56−63**. Glacial acetic acid (2 mL) was added to a suspension of **39−46** (1.0 mmol) in THF. $NaBH_4$ (5.0 mmol) was then added in small portions, cooling the solution in an ice bath. The mixture was heated at 60 °C under nitrogen for 4 h. After cooling, $H_2O$ was added, and the solution was made acidic with 3 N HCl and washed with ether. The aqueous phase was then basified with NaOH pellets and extracted with $CH_2Cl_2$. The dried solvents were evaporated to afford the desired compounds. **61−63** were purified by flash chromatography.

**[6-(Benzylethylamino)hexyl]carbamic Acid Benzyl Ester (56)**. **56** was obtained from **39**: colorless oil; 75% yield.

{**6-[Ethyl(4-methoxybenzyl)amino]hexyl**}**carbamic Acid Benzyl Ester (57)**. **57** was obtained from **40**: yellow oil; 71% yield.

{**6-[Ethyl(3-methoxybenzyl)amino]hexyl**}**carbamic Acid Benzyl Ester (58)**. **58** was obtained from **41**: colorless oil; 60% yield.

{**6-[Ethyl(furan-2-ylmethyl)amino]hexyl**}**carbamic Acid Benzyl Ester (59)**. **59** was obtained from **42**: yellow oil; 60% yield.

{**6-[Ethyl(thiophen-2-ylmethyl)amino]hexyl**}**carbamic Acid Benzyl Ester (60)**. **60** was obtained from **43**: yellow oil; 70% yield.

{**6-[Ethyl(pyridin-2-ylmethyl)amino]hexyl**}**carbamic Acid Benzyl Ester (61)**. **61** was obtained from **44**: eluent EtOAc/toluene/EtOH/aqueous 28% ammonia (7:3:0.5:0.05); yellow oil; 40% yield.

{**6-[Ethyl(pyridin-3-ylmethyl)amino]hexyl**}**carbamic Acid Benzyl Ester (62)**. **62** was obtained from **45**: eluent EtOAc/toluene/EtOH/aqueous 28% ammonia (7:3:0.5:0.05); yellow oil; 40% yield

{**6-[Ethyl(pyridin-4-ylmethyl)amino]hexyl**}**carbamic Acid Benzyl Ester (63)**. **63** was obtained from **46**: eluent EtOAc/$CH_2Cl_2$/EtOH/aqueous 28% ammonia (6:4:0.5:0.05); yellow oil; 40% yield.

{**6-[(2-Methoxyphenyl)methylamino]hexyl**}**carbamic Acid Benzyl Ester (64)**. To a suspension of **34** (5.0 g, 13.5 mmol) in $H_2O$ (25 mL) were added 95% HCOOH (1.6 mL, 40.5 mmol) and 37% HCHO (3.1 mL, 40.5 mmol). The mixture was refluxed for 6 h and then stirred at room temperature overnight. After partial evaporation of the solvent, the resulting suspension was made basic with 40% NaOH and extracted with $CHCl_3$ (3 × 100 mL). The dried extracts were evaporated to afford a residue which was purified by flash chromatography. Elution with $CHCl_3$/petroleum ether/MeOH/aqueous 28% ammonia (8:2:0.7:0.05) afforded **64**: pale yellow oil; 75% yield.

**General Procedure for the Synthesis of 65−83**. A solution of 30% HBr in $CH_3COOH$ (6.5 mL) was added to a solution of **47−64** or **34** (1.0 mmol) in $CH_3COOH$, and the resulting mixture was stirred overnight at room temperature. Ether was then added, and the resulting oil was washed with ether and dissolved in $H_2O$. The solution was made basic with NaOH pellets and extracted with $CHCl_3$. Removal of the dried solvents afforded the desired compounds.

***N*1-Ethyl-*N*1-(2-methoxybenzyl)ethane-1,2-diamine (65)**. **65** was obtained from **47**: colorless oil; quantitative yield.

***N*1-Ethyl-*N*1-(2-methoxybenzyl)propane-1,3-diamine (66)**. **66** was obtained from **48**: colorless oil; quantitative yield.

***N*1-Ethyl-*N*1-(2-methoxybenzyl)butane-1,4-diamine (67)**. **67** was obtained from **49**: yellow oil; quantitative yield.

***N*1-Ethyl-*N*1-(2-methoxybenzyl)pentane-1,5-diamine (68)**. **68** was obtained from **50**: yellow oil; 70% yield.

***N*1-Ethyl-*N*1-(2-methoxybenzyl)hexane-1,6-diamine (69)**. **69** was obtained from **51**: yellow oil; 90% yield.

***N*1-Ethyl-*N*1-(2-methoxybenzyl)heptane-1,7-diamine (70)**. **70** was obtained from **52**: yellow oil; quantitative yield.

***N*1-Ethyl-*N*1-(2-methylbenzyl)hexane-1,6-diamine (71)**. **71** was obtained from **53**: yellow oil; 90% yield.

***N*1-(2-Chlorobenzyl)-*N*1-ethylhexane-1,6-diamine (72)**. **72** was obtained from **54**: yellow oil; quantitative yield.

***N*1-Ethyl-*N*1-(2-nitrobenzyl)hexane-1,6-diamine (73)**. **73** was obtained from **55**: yellow oil; quantitative yield.

***N*1-(2-Methoxybenzyl)hexane-1,6-diamine (74)**. **74** was obtained from **34**:[23] yellow oil; 65% yield.

***N*1-Benzyl-*N*1-ethylhexane-1,6-diamine (75)**. **75** was obtained from **56**: yellow oil; quantitative yield.

***N*1-Ethyl-*N*1-(4-methoxybenzyl)hexane-1,6-diamine (76)**. **76** was obtained from **57**: yellow oil; 90% yield.

***N*1-Ethyl-*N*1-(3-methoxybenzyl)hexane-1,6-diamine (77)**. **77** was obtained from **58**: yellow oil; quantitative yield.

***N*1-Ethyl-*N*1-(furan-2-ylmethyl)hexane-1,6-diamine (78)**. **78** was obtained from **59**: colorless oil; 85% yield.

***N*1-Ethyl-*N*1-(thiophen-2-ylmethyl)hexane-1,6-diamine (79)**. **79** was obtained from **60**: yellow oil; 80% yield.

***N*1-Ethyl-*N*1-(pyridin-2-ylmethyl)hexane-1,6-diamine (80)**. **80** was obtained from **61**: colorless oil; 75% yield.

***N*1-Ethyl-*N*1-(pyridin-3-ylmethyl)hexane-1,6-diamine (81)**. **81** was obtained from **62**: colorless oil; 75% yield.

***N*1-Ethyl-*N*1-(pyridin-4-ylmethyl)hexane-1,6-diamine (82)**. **82** was obtained from **63**: colorless oil; 75% yield.

***N*1-(2-Methoxybenzyl)-*N*1-methylhexane-1,6-diamine (83)**. **83** was obtained from **64**: yellow oil; quantitative yield.

**(6-**{**Ethyl[2-(2-methoxyphenyl)ethyl]amino**}**hexyl)carbamic Acid *tert*-Butyl Ester (84)**. Some crystals of KI and a solution of *N*-ethyl-*N*-(2-methoxy)phenethylamine[26] (2.4 g, 1.2 mmol) in DMF (5 mL) were added to a solution of (6-chlorohexyl)carbamic acid *tert*-butyl ester[27] (1.0 g, 5.6 mmol) and $Et_3N$ (1.3 mL, 11.2 mmol) in DMF (10 mL). The resulting mixture was heated at 105 °C for 48 h, and then the solvent was removed to give a residue that was partitioned between $H_2O$ and $CHCl_3$. The dried organic fraction was evaporated, affording an oil that was purified by flash chromatography. Elution with $CH_2Cl_2$/petroleum ether/EtOH/aqueous 28% ammonia (9:1:0.4:0.07) afforded the desired compound: yellow oil; 35% yield.

***N*1-Ethyl-*N*1-[2-(2-methoxyphenyl)ethyl]hexane-1,6-diamine (85)**. A solution of $CF_3COOH$ (4.5 mL) and **84** (0.75 g, 1.98 mmol) in $CHCl_3$ (20 mL) was stirred at room temperature for 2 h. After removal of the solvent, the residue was dissolved in $H_2O$, washed with ether (2 × 50 mL), basified with 40% NaOH, and extracted with $CHCl_3$ (3 × 60 mL). Removal of the organic phase afforded **85**: yellow oil; 85% yield.

{**5-[Ethyl(2-methoxybenzyl)carbamoyl]pentyl**}**carbamic Acid Benzyl Ester (86)**. Ethyl chlorocarbonate (0.95 mL, 10.0 mmol) in dry dioxane (3 mL) was added dropwise to a stirred and cooled solution of *N*-Z-6-aminocaproic acid (2.65 g, 10.0 mmol) and $Et_3N$ (1.4 mL, 10.0 mmol) in dioxane (60 mL), followed, after the resulting solution was allowed to stand for 20 min, by the addition of *N*-ethyl-*N*-(2-methoxy)benzylamine[28] (1.65 g, 10.0 mmol) in dioxane (10 mL). After being stirred at room temperature overnight, the mixture was evaporated, affording a residue that was suspended in water (150 mL). The precipitate was filtered and washed with 2 N $KHSO_4$, aqueous $NaHCO_3$ saturated solution, and water to give **86**: 66% yield.

**6-Aminohexanoic Acid Ethyl(2-methoxybenzyl)amide (87)**. A solution of **86** (1.12 g, 14 mmol) in methanol (60 mL) was hydrogenated over 10% Pd on charcoal (0.11 g) for 1 h at room temperature and a pressure of 15 psi. Following catalyst removal, the solvent was evaporated, affording **87**: colorless oil; quantitative yield.

**[6-(Isopropylamino)hexyl]carbamic Acid Benzyl Ester (88)**. Acetone (0.45 mL, 6.0 mmol) was added to a solution of (6-aminohexyl)carbamic acid benzyl ester (0.50 g, 2.0 mmol) in EtOH (10 mL). The resulting solution was stirred for 10 min followed by the addition of $NaBH_4$ (0.23 g, 6.0 mmol) and heating at 60 °C for 48 h. After removal of the solvent, the residue was purified by flash chromatography. Eluting with $CHCl_3$/MeOH/aqueous 28% ammonia (9:1:0.8) afforded the desired compound: colorless oil; 78% yield.

{**6-[Isopropyl(2-methoxybenzyl)amino]hexyl**}**carbamic Acid Benzyl Ester (89)**. $Et_3N$ (0.45 mL), some crystals of KI, and, dropwise, a solution of 2-methoxybenzyl chloride (0.28 mL, 2.06

mmol) in DMF (3 mL) were added to a solution of **88** (0.30 g, 1.03 mmol) in DMF (4 mL). The mixture was heated at 105 °C for 4 days. The solvent was removed, and the residue was partitioned between $H_2O$ and $CHCl_3$. The dried organic fraction was evaporated, affording an oil which was purified by flash chromatography. Elution with $CHCl_3$/EtOH (9.7:0.3) afforded **89**: brown oil; 50% yield.

***N*1-Isopropyl-*N*1-(2-methoxybenzyl)hexane-1,6-diamine (90)**. **90** was obtained from **89** following the procedure described for **65**−**83**: yellow oil; 70% yield.

**General Procedure for the Synthesis of 3**−**5**. A suspension of the proper 2,3,5,6-tetrahalogeno-*p*-benzoquinone (0.56 mmol) in ether (2 mL) was added dropwise to a solution of **69** (1.23 g, 4.66 mmmol) in ether (3 mL). The reaction mixture turned a dark red color almost immediately. After the reaction mixture was stirred for 1 h at room temperature, the solvent was evaporated under vacuum. The residue was then purified by flash chromatography.

**Data for 2,5-bis{6-[ethyl(2-methoxybenzyl)amino]hexylamino}-3,6-difluoro-[1,4]-benzoquinone (3)**: eluent $CH_2Cl_2$/MeOH/aqueous 28% ammonia (9:1:0.05); green oil; 90% yield; $^1$H NMR (free base, $CDCl_3$) $\delta$ 1.08 (t, 6H), 1.23−1.63 (m complex, 16H), 2.46−2.64 (m, 8H), 3.51 (q, 4H), 3.64 (s, 4H), 3.84 (s, 6H), 6.17 (br s, 2H exchangeable with $D_2O$), 6.87 (d, 2H), 6.95 (t, 2H), 7.24 (t, 2H), 7.43 (d, 2H); MS (ESI$^+$) $m/z$ = 669 (M + H)$^+$. Anal. ($C_{38}H_{54}F_2N_4O_4$) C, H, N.

**Data for 2,5-bis{6-[ethyl(2-methoxybenzyl)amino]hexylamino}-3,6-dichloro-[1,4]-benzoquinone (4)**: eluent $CH_2Cl_2$/MeOH/aqueous 28% ammonia (9:1:0.05); violet oil; 35% yield; $^1$H NMR (free base, $CDCl_3$) $\delta$ 1.08 (t, 6H), 1.28−1.78 (m complex, 16H), 2.42−2.63 (m, 8H), 3.63 (s, 4H), 3.75−3.86 (m, 10H), 6.85 (d, 2H), 6.94 (t, 2H), 7.12 (br s, 2H exchangeable with $D_2O$), 7.22 (t, 2H), 7.43 (d, 2H); MS (ESI$^+$) $m/z$ = 701 (M + H)$^+$. Anal. ($C_{38}H_{54}Cl_2N_4O_4$) C, H, N.

**Data for 2,5-bis{6-[ethyl(2-methoxybenzyl)amino]hexylamino}-3,6-dibromo-[1,4]-benzoquinone (5)**: eluent $CH_2Cl_2$/MeOH/aqueous 28% ammonia (9:1:0.05); violet oil; 25% yield; $^1$H NMR (free base, $CDCl_3$) $\delta$ 1.07 (t, 6H), 1.28−1.78 (m complex, 16H), 2.43−2.60 (m, 8H), 3.60 (s, 4H), 3.84−3.94 (m, 10H), 6.87 (d, 2H), 6.95 (t, 2H), 7.19−7.28 (m, 2H + 2H exchangeable with $D_2O$), 7.42 (d, 2H); MS (ESI$^+$) $m/z$ = 791 (M + H)$^+$. Anal. ($C_{38}H_{54}Br_2N_4O_4$) C, H, N.

**2,5-Bis{6-[ethyl(2-methoxybenzyl)amino]hexylamino}-3,6-dimethyl-[1,4]-benzoquinone (6) and 2,5-Bis{6-[ethyl(2-methoxybenzyl)amino]hexylamino}-3,6-diphenyl-[1,4]-benzoquinone (7)**. A solution of diamine **69** (2.1 mmol) was added dropwise to a suspension of the appropriate 3,6-disubstituted 1,4-benzoquinone (1.0 mmol). The reaction solvent was MeOH for **6** and EtOH for **7**. The solution was stirred (room temperature and 60 °C, respectively), and the state of the reaction was continuously monitored by TLC. After removal of the solvent, the residue was purified by gravity chromatography.

**Data for 6**: eluent $CH_2Cl_2$/MeOH/aqueous 28% ammonia (9.5:0.5:0.04); purple oil; 10% yield; $^1$H NMR (free base, $CDCl_3$) $\delta$ 1.08 (t, 6H), 1.29−1.63 (m, 16H), 2.07 (s, 6H), 2.48−2.60 (m, 8H), 3.53 (q, 4H), 3.64 (s, 4H), 3.85 (s, 6H), 6.73 (br t, 2H exchangeable with $D_2O$), 6.85−6.97 (m, 4H), 7.28 (t, 2H), 7.45 (d, 2H); MS (ESI$^+$) $m/z$ = 661 (M + H)$^+$. Anal. ($C_{40}H_{60}N_4O_4$) C, H, N.

**Data for 7**: eluent $CH_2Cl_2$/MeOH/aqueous 28% ammonia (9.25:0.75:0.075); pink solid; mp 104 °C (ether); 19% yield; $^1$H NMR (free base, $CDCl_3$) $\delta$ 1.01−1.83 (m complex, 22H), 2.36−2.69 (m complex, 12H), 3.58 (s, 4H), 3.82 (s, 6H) 6.83−6.97 (m complex, 4H + 2H exchangeable with $D_2O$), 7.19−7.40 (m complex, 14H); MS (ESI$^+$) $m/z$ = 786 (M + H)$^+$. Anal. ($C_{50}H_{64}N_4O_4$) C, H, N.

**General Procedure for the Synthesis of 2 and 9**−**29**. A solution of **69** (12.2 g, 46 mmol) in EtOH (150 mL) was added dropwise to a suspension of 2,5-dimethoxyquinone (3.85 g; 23.0 mmol) in boiling EtOH (450 mL). The reaction mixture became progressively clear and red. It was heated at 60 °C for 5 h and, after cooling, filtered through a paper filter. The filtrate was concentrated under vacuum to give **2** (2,5-bis{6-[ethyl(2-methoxybenzyl)amino]hexylamino}-[1,4]-benzoquinone) as a red solid in quantitative yield, which was identical to that obtained by a different synthetic scheme.[23]

Compounds **9**−**29** were synthesized using the same procedure.

**2,5-Bis{2-[ethyl(2-methoxybenzyl)amino]ethylamino}-[1,4]-benzoquinone (9)**. **9** was obtained from **65**: eluent petroleum ether/EtOAc/MeOH/aqueous 28% ammonia (7:3:0.4:0.03); red-brown solid; mp 127−130 °C; 60% yield; $^1$H NMR (free base, $CD_3OD$) $\delta$ 1.15 (t, 6H), 2.64 (q, 4H), 2.79 (t, 4H), 3.18−3.25 (m, 4H), 3.71 (s, 4H), 3.82 (s, 6H), 5.28 (s, 2H), 6.88−6.99 (m, 4H), 7.21−7.38 (m, 4H); MS (ESI$^+$) $m/z$ = 521 (M + H)$^+$. Anal. ($C_{30}H_{40}N_4O_4$) C, H, N.

**2,5-Bis{3-[ethyl(2-methoxybenzyl)amino]propylamino}-[1,4]-benzoquinone (10)**. **10** was obtained from **66**: eluent $CH_2Cl_2$/MeOH/aqueous 28% ammonia (9.75:0.25:0.025); foam red solid; 85% yield; $^1$H NMR (free base, $CDCl_3$) $\delta$ 1.11 (t, 6H), 1.72−1.85 (m, 4H), 2.56 (q, 8H), 3.18 (q, 4H), 3.62 (s, 4H), 3.82 (s, 6H), 5.26 (s, 2H), 6.83−6.95 (m, 4H), 7.19−7.43 (m, 4H + 2H exchangeable with $D_2O$); MS (ESI$^+$) $m/z$ = 549 (M + H)$^+$. Anal. ($C_{32}H_{44}N_4O_4$) C, H, N.

**2,5-Bis{4-[ethyl(2-methoxybenzyl)amino]butylamino}-[1,4]-benzoquinone (11)**. **11** was obtained from **67**: red solid; mp 97 °C (EtOH); 72% yield; $^1$H NMR (free base, $CDCl_3$) $\delta$ 1.08 (t, 6H), 1.51−1.77 (m, 8H), 2.42−2.63 (m, 8H), 3.11 (q, 4H), 3.60 (s, 4H), 3.81 (s, 6H), 5.28 (s, 2H), 7.72 (br t, 2H exchangeable with $D_2O$), 6.82−7.01 (m, 4H), 7.19−7.23 (m, 2H), 7.38−7.42 (m, 2H); MS (ESI$^+$) $m/z$ = 577 (M + H)$^+$. Anal. ($C_{34}H_{48}N_4O_4$) C, H, N.

**2,5-Bis{5-[ethyl(2-methoxybenzyl)amino]pentylamino}-[1,4]-benzoquinone (12)**. **12** was obtained from **68**: red solid (EtOH); mp 88 °C; 68% yield; $^1$H NMR (free base, $CDCl_3$) $\delta$ 1.18 (t, 6H), 1.28−1.72 (m, 12H), 2.43−2.61 (m, 8H), 3.15 (q, 4H), 3.62 (s, 4H), 3.84 (s, 6H), 5.33 (s, 2H), 6.61 (br t, 2H exchangeable with $D_2O$), 6.86−7.01 (m, 4H), 7.22−7.29 (m, 2H), 7.42−7.46 (m, 2H); MS (ESI$^+$) $m/z$ = 605 (M + H)$^+$. Anal. ($C_{36}H_{52}N_4O_4$) C, H, N.

**2,5-Bis{7-[ethyl(2-methoxybenzyl)amino]heptylamino}-[1,4]-benzoquinone (13)**. **13** was obtained from **70**: eluent $CHCl_3$/petroleum ether/MeOH/aqueous 28% ammonia (8:1:1:0.08); red oil; 62% yield; $^1$H NMR (free base, $CDCl_3$) $\delta$ 1.08 (t, 6H), 1.28−1.42 (m, 12H), 1.45−1.60 (m, 4H), 1.62−1.75 (m, 4H), 2.48 (t, 4H), 2.58 (q, 4H), 3.18 (q, 4H), 3.62 (s, 4H), 3.83 (s, 6H), 5.35 (s, 2H), 6.62 (br t, 2H exchangeable with $D_2O$), 6.85−6.90 (m, 2H), 6.97 (t, 2H), 7.22 (t, 2H), 7.43 (d, 2H); MS (ESI$^+$) $m/z$ = 661 (M + H)$^+$. Anal. ($C_{40}H_{60}N_4O_4$) C, H, N.

**2,5-Bis(6-{ethyl[2-(2-methoxyphenyl)ethyl]amino}hexylamino)-[1,4]-benzoquinone (14)**. **14** was obtained from **85**: foam red solid (EtOH); 75% yield; $^1$H NMR (free base, $CDCl_3$) $\delta$ 1.03 (t, 6H), 1.23−1.68 (m, 22H), 2.39−2.75 (m, 8H), 3.16 (q, 4H), 3.81 (s, 6H), 4.32 (q, 2H), 5.31 (s, 2H), 6.61 (t, 2H exchangeable with $D_2O$), 6.83−7.01 (m, 4H), 7.17−7.29 (m, 2H), 7.39−7.48 (m, 2H); MS (ESI$^+$) $m/z$ = 661 (M + H)$^+$. Anal. ($C_{40}H_{60}N_4O_4$) C, H, N.

**6-(4-{5-[Ethyl(2-methoxybenzyl)carbamoyl]pentylamino}-3,6-dioxocyclohexa-1,4-dienylamino)hexanoic Acid Ethyl(2-methoxybenzyl)amide (15)**. **15** was obtained from **87**: red solid ($Et_2O$); mp 134 °C; 65% yield; $^1$H NMR (free base, $CDCl_3$) $\delta$ 1.11−1.21 (m, 6H), 1.28−1.76 (m complex, 12H), 2.34 (t, 2.4 H), 2.44 (t, 1.6H), 3.11−3.23 (m, 4H), 3.34 (q, 1.6H), 3.46 (q, 2.4H), 3.87 (s, 2.4H), 3.90 (s, 3.6), 4.53 (s, 2.4H), 4.64 (s, 1.6H), 5.30−5.33 (d, 2H), 6.59 (br s, 2H exchangeable with $D_2O$), 6.82−7.32 (m, 8H); MS (ESI$^+$) $m/z$ = 683 (M + Na)$^+$. Anal. ($C_{38}H_{52}N_4O_6$) C, H, N.

**2,5-Bis[6-(2-methoxybenzylamino)hexylamino]-[1,4]-benzoquinone (16)**. **16** was obtained from **74**: red solid (EtOH); mp 205 °C; quantitative yield; $^1$H NMR (free base, $CDCl_3$) $\delta$ 1.28−1.42 (m, 8H), 1.52−1.76 (m, 8H), 2.63 (t, 4H), 3.16 (q, 4H), 3.78−3.85 (m, 10H + 2H exchangeable with $D_2O$), 5.32 (s, 2H), 6.62 (br t, 2H exchangeable with $D_2O$), 6.85−6.96 (m, 4H), 7.22−7.35 (m, 4H); MS (ESI$^+$) $m/z$ = 577 (M + H)$^+$. Anal. ($C_{34}H_{48}N_4O_4$) C, H, N.

**2,5-Bis{6-[(2-methoxybenzyl)methylamino]hexylamino}-[1,4]-benzoquinone (17)**. **17** was obtained from **83**: eluent $CH_2Cl_2$/petroleum ether/EtOH/aqueous 28% ammonia (9:1:0.6:0.05); foam red solid; 77% yield; $^1$H NMR (free base, $CDCl_3$) $\delta$ 1.31−1.48

(m, 16H), 2.22 (s, 6H), 2.41 (t, 4H), 3.15 (q, 4H), 3.52 (s, 4H), 3.83 (s, 6H), 5.32 (s, 2H), 6.62 (br t, 2H exchangeable with $D_2O$), 6.83−6.99 (m, 4H), 7.19−7.38 (m, 4H); MS ($ESI^+$) $m/z$ = 605 $(M + H)^+$. Anal. ($C_{36}H_{52}N_4O_4$) C, H, N.

**2,5-Bis{6-[isopropyl(2-methoxybenzyl)amino]hexylamino}-[1,4]-benzoquinone (18)**. **18** was obtained from **90**: red solid (EtOH); mp 116 °C; 80% yield; $^1H$ NMR (free base, $CDCl_3$) $\delta$ 1.05 (d, 12H), 1.34−1.48 (m, 12H), 1.59−1.70 (m, 4H), 2.46 (t, 4H), 2.97 (sept, 2H), 3.14 (q, 4H), 3.60 (s, 4H), 3.85 (s, 6H), 5.32 (s, 2H), 6.60 (br t, 2H exchangeable with $D_2O$), 6.83−6.89 (m, 2H), 6.87 (t, 2H), 7.23 (t, 2H), 7.58 (d, 2H); MS ($ESI^+$) $m/z$ = 660 $(M + H)^+$. Anal. ($C_{40}H_{60}N_4O_4$) C, H, N.

**2,5-Bis[6-(benzylethylamino)hexylamino]-[1,4]-benzoquinone (19)**. **19** was obtained from **75**: eluent $CH_2Cl_2$/EtOH/aqueous 28% ammonia (9.5:0.5:0.07); foam red solid; 82% yield; $^1H$ NMR (free base, $CDCl_3$) $\delta$ 1.05 (t, 6H), 1.14−1.39 (m, 8H), 1.43−1.53 (m, 4H), 1.58−1.65 (m, 4H), 2.41−2.56 (m, 8H), 3.10 (q, 4H), 3.71 (s, 4H), 5.28 (s, 2H), 6.44 (br t, 2H exchangeable with $D_2O$), 7.10−7.24 (m, 10H); MS ($ESI^+$) $m/z$ = 573 $(M + H)^+$. Anal. ($C_{36}H_{52}N_4O_2$) C, H, N.

**2,5-Bis{6-[ethyl(4-methoxybenzyl)amino]hexylamino}-[1,4]-benzoquinone (20)**. **20** was obtained from **76**: eluent $CH_2Cl_2$/petroleum ether/EtOH/aqueous 28% ammonia (8:1:1:0.05); foam red solid; 79% yield; $^1H$ NMR (free base, $CDCl_3$) $\delta$ 1.04 (t, 6H), 1.22−1.56 (m, 12H), 1.58−1.72 (m, 4H), 2.38−2.56 (m, 8H), 3.12 (q, 4H), 3.47 (s, 4H), 3.79 (s, 6H), 5.32 (s, 2H), 6.59 (br t, 2H exchangeable with $D_2O$), 6.82−6.93 (m, 4H), 7.21−7.30 (m, 4H); MS ($ESI^+$) $m/z$ = 633 $(M + H)^+$. Anal. ($C_{38}H_{56}N_4O_4$) C, H, N.

**2,5-Bis{6-[ethyl(3-methoxybenzyl)amino]hexylamino}-[1,4]-benzoquinone (21)**. **21** was obtained from **77**: eluent $CH_2Cl_2$/petroleum ether/EtOH/aqueous 28% ammonia (8:1:1:0.05); foam red solid; 75% yield; $^1H$ NMR (free base, $CDCl_3$) $\delta$ 1.04 (t, 6H), 1.24−1.57 (m, 12H), 1.60−1.75 (m, 4H), 2.39−2.60 (m, 8H), 3.09 (q, 4H), 3.57 (s, 4H), 3.81 (s, 6H), 5.32 (s, 2H), 6.63 (br t, 2H exchangeable with $D_2O$), 6.76−6.95 (m, 6H), 7.18−7.28 (t, 2H); MS ($ESI^+$) $m/z$ = 633 $(M + H)^+$. Anal. ($C_{38}H_{56}N_4O_4$) C, H, N.

**2,5-Bis{6-[ethyl(2-methylbenzyl)amino]hexylamino}-[1,4]-benzoquinone (22)**. **22** was obtained from **71**: eluent $CH_2Cl_2$/petroleum ether/EtOH/aqueous 28% ammonia (7:3:0.3:0.035); foam red solid; 78% yield; $^1H$ NMR (free base, $CDCl_3$) $\delta$ 1.03 (t, 6H), 1.22−1.73 (m, 16H), 2.28−2.58 (m, 14H), 3.12 (q, 4H), 3.55 (s, 4H), 5.32 (s, 2H), 6.61 (br t, 2H exchangeable with $D_2O$), 7.12−7.21 (m, 6H), 7.25−7.40 (m, 2H); MS ($ESI^+$) $m/z$ = 601 $(M + H)^+$. Anal. ($C_{38}H_{56}N_4O_2$) C, H, N.

**2,5-Bis{6-[(2-chlorobenzyl)ethylamino]hexylamino}-[1,4]-benzoquinone (23)**. **23** was obtained from **72**: red solid (EtOH); mp 70 °C; 64% yield; $^1H$ NMR (free base, $CDCl_3$) $\delta$ 1.04 (t, 6H), 1.10−1.35 (m, 8H), 1.43−1.53 (m, 4H), 1.57−1.65 (m, 4H), 2.41−2.56 (m, 8H), 3.08 (q, 4H), 3.46 (s, 4H), 5.31 (s, 2H), 6.59 (br t, 2H exchangeable with $D_2O$), 7.05−7.23 (m, 6H), 7.45 (d, 2H); MS ($ESI^+$) $m/z$ = 641 $(M + H)^+$. Anal. ($C_{36}H_{50}Cl_2N_4O_2$) C, H, N.

**2,5-Bis{6-[ethyl(2-nitrobenzyl)amino]hexylamino}-[1,4]-benzoquinone (24)**. **24** was obtained from **73**: eluent $CH_2Cl_2$/petroleum ether/EtOH/aqueous 28% ammonia (8:2:0.5:0.035); foam red solid; 61% yield; $^1H$ NMR (free base, $CDCl_3$) $\delta$ 0.98 (t, 6H), 1.19−1.50 (m, 12H), 1.52−1.72 (m, 4H), 2.35−2.57 (m, 8H), 3.13 (q, 4H), 3.83 (s, 4H), 5.30 (s, 2H), 6.58−6.66 (br t, 2H exchangeable with $D_2O$), 7.32−7.41 (m, 2H), 7.48−7.58 (m, 2H), 7.62−7.70 (m, 2H), 7.78−7.82 (m, 2H); MS ($ESI^+$) $m/z$ = 663 $(M + H)^+$. Anal. ($C_{36}H_{50}N_6O_6$) C, H, N.

**2,5-Bis{6-[ethyl(furan-2-ylmethyl)amino]hexylamino}-[1,4]-benzoquinone (25)**. **25** was obtained from **78**: eluent $CH_2Cl_2$/EtOH/aqueous 28% ammonia (9.5:0.5:0.07); foam red solid; 80% yield; $^1H$ NMR (free base, $CDCl_3$) $\delta$ 1.09 (t, 6H), 1.22−1.58 (m, 12H), 1.60−1.73 (m, 4H), 2.43 (t, 4H), 2.57 (q, 4H), 3.18 (q, 4H), 3.63 (s, 4H), 5.32 (s, 2H), 6.18−6.22 (m, 2H), 6.32−6.39 (m, 2H), 6.62 (br t, 2H exchangeable with $D_2O$), 7.38−7.41 (m, 2H); MS ($ESI^+$) $m/z$ = 553 $(M + H)^+$. Anal. ($C_{32}H_{48}N_4O_4$) C, H, N.

**2,5-Bis{6-[ethyl(thiophen-2-ylmethyl)amino]hexylamino}-[1,4]-benzoquinone (26)**. **26** was obtained from **79**: red solid; mp 55 °C ($H_2O$/EtOH); 85% yield; $^1H$ NMR (free base, $CDCl_3$) $\delta$ 1.08 (t, 6H), 1.35−1.75 (m, 16H), 2.41−2.62 (m, 8H), 3.18 (q, 4H), 3.81 (s, 4H), 5.38 (s, 2H), 6.62 (br s, 2H exchangeable with $D_2O$), 6.88−7.00 (m, 4H), 7.21−7.25 (m, 2H); MS ($ESI^+$) $m/z$ = 585 $(M + H)^+$. Anal. ($C_{32}H_{48}N_4O_2S_2$) C, H, N.

**2,5-Bis{6-[ethyl(pyridin-2-ylmethyl)amino]hexylamino}-[1,4]-benzoquinone (27)**. **27** was obtained from **80**: foam red solid ($H_2O$/EtOH); 60% yield; $^1H$ NMR (free base, $CDCl_3$) $\delta$ 1.02 (t, 6H), 1.18−1.68 (m, 16H), 2.38−2.60 (m, 8H), 3.12 (q, 4H), 3.64 (s, 4H), 5.22 (s, 2H), 6.60 (br s, 2H exchangeable with $D_2O$), 7.08−7.17 (m, 2H), 7.40−7.48 (m, 2H), 7.57−7.68 (m, 2H), 8.42−8.48 (m, 2H); MS ($ESI^+$) $m/z$ = 575 $(M + H)^+$. Anal. ($C_{34}H_{50}N_6O_2$) C, H, N.

**2,5-Bis{6-[ethyl(pyridin-3-ylmethyl)amino]hexylamino}-[1,4]-benzoquinone (28)**. **28** was obtained from **81**: foam red solid ($H_2O$/EtOH); 50% yield; $^1H$ NMR (free base, $CDCl_3$) $\delta$ 1.02 (t, 6H), 1.22−1.66 (m, 16H), 2.33−2.56 (m, 8H), 3.12 (q, 4H), 3.53 (s, 4H), 5.25 (s, 2H), 6.62 (br s, 2H exchangeable with $D_2O$), 7.19−7.24 (m, 2H), 7.62−7.68 (m, 2H), 7.57−7.68 (m, 2H), 8.41−8.55 (m, 2H); MS ($ESI^+$) $m/z$ = 575 $(M + H)^+$. Anal. ($C_{34}H_{50}N_6O_2$) C, H, N.

**2,5-Bis{6-[ethyl(pyridin-4-ylmethyl)amino]hexylamino}-[1,4]-benzoquinone (29)**. **29** was obtained from **82**: eluent $CH_2Cl_2$/EtOH/aqueous 28% ammonia (9.5:1:0.06); foam red solid; 67% yield; $^1H$ NMR (free base, $CDCl_3$) $\delta$ 0.98 (t, 6H), 1.22−1.75 (m, 16H), 2.35−2.58 (m, 8H), 3.12 (q, 4H), 3.52 (s, 4H), 5.25 (s, 2H), 6.63 (br s, 2H exchangeable with $D_2O$), 7.21−7.28 (m, 4H), 8.42−8.48 (m, 4H); MS ($ESI^+$) $m/z$ = 575 $(M + H)^+$. Anal. ($C_{34}H_{50}N_6O_2$) C, H, N.

**{5-[4-(6-Benzyloxycarbonylaminohexanoylamino)-phenylcarbamoyl]pentyl}carbamic Acid Benzyl Ester (91)**. **91** was obtained from ethyl chlorocarbonate (0.72 mL, 7.24 mmol), *N*-Z-6-aminocaproic acid (1.0 mL, 7.24 mmol), $Et_3N$ (2.0 g, 7.24 mmol), and 1,4-phenylenediamine (0.41 g, 3.77 mmol) following the procedure described for **86**. After being stirred at room temperature overnight, the mixture was poured into water, affording a white solid which was collected by filtration and washed with 1 N HCl, 1 N NaOH, and water to give **91**: 70% yield; mp 195 °C dec.

**6-Aminohexanoic Acid [4-(6-Aminohexanoylamino)phenyl]-amide (92)**. **92** was obtained from **91** (1.53 g, 2.55 mmol) following the procedure described for **65**−**83**: white solid; mp 160−165 °C; 85% yield.

**6-(2-Methoxybenzylamino)hexanoic Acid {4-[6-(2-Methoxybenzylamino)hexanoylamino]phenyl}amide (93)**. **93** was obtained from **92** (0.70 g, 2.09 mmol) and 2-methoxybenzaldehyde (0.63 g, 4.6 mmol) following the procedure described for **30**−**46**: oil; 75% yield.

**6-[Ethyl(2-methoxybenzyl)amino]hexanoic Acid (4-{6-[Ethyl-(2-methoxybenzyl)amino]hexanoylamino}phenyl)amide (94)**. **94** was obtained from **93** (0.86 g, 1.50 mmol) following the procedure described for **47**−**55** and purified by gravity chromatography. Eluting with $CHCl_3$/MeOH/aqueous 28% ammonia (9:1:0.05) gave the desired compound: yellow oil; 32% yield.

***N,N′*-Bis{6-[ethyl(2-methoxybenzyl)amino]hexyl}benzene-1,4-diamine (8)**. A solution of 10 M $BH_3{\cdot}CH_3SCH_3$ (0.15 mL) in dry diglyme (10 mL) was added dropwise at room temperature to a solution of **94** (0.30 g, 0.47 mmol) in dry diglyme (20 mL) with stirring under a stream of dry nitrogen. When the addition was completed, the reaction mixture was heated at 120 °C for 8 h. After the reaction mixture was cooled at 0 °C, excess borane was destroyed by cautious dropwise addition of MeOH (10 mL). The resulting mixture was left to stand overnight at room temperature, cooled at 0 °C, treated with HCl gas for 30 min, and then heated at 120 °C for 5 h. After cooling, ether was added and the resulting solid collected by filtration and dissolved in water. The aqueous phase was washed with ether, made basic with 3 N NaOH, and extracted with $CHCl_3$. Removal of the dried solvent gave a residue that was purified by gravity column chromatography. Elution with $CH_2Cl_2$/EtOH/aqueous 28% ammonia (9:1:0.02) afforded **8**: dark red oil; 50% yield; $^1H$ NMR (free base, $CDCl_3$) $\delta$ 1.12 (t, 6H), 1.28−1.48 (m, 8H + 2H exchangeable with $D_2O$), 1.50−1.68 (m,

8H), 2.52 (t, 4H), 2.59 (q, 4H), 3.06 (t, 4H), 3.63 (s, 4H), 3.82 (s, 6H), 6.58 (s, 4H), 6.88−6.90 (m, 2H), 6.93−7.01 (m, 2H), 7.22−7.32 (m, 2H), 7.43−7.48 (m, 2H); MS (ESI$^+$) $m/z$ = 603 (M + H)$^+$. Anal. ($C_{38}H_{58}N_4O_2$) C, H, N.

**Determination of the Inhibitory Effect on AChE and BChE Activities**. The method of Ellman et al.[54] was followed. Prototypes **1** and **2** and the AChEIs tacrine, donepezil, galantamine, and rivastigmine were used as reference compounds. Five different concentrations of each compound were used to obtain inhibition of AChE or BChE activity comprised between 20% and 80%. The assay solution consisted of a 0.1 M phosphate buffer, pH 8.0, with the addition of 340 $\mu$M 5,5′-dithiobis(2-nitrobenzoic acid), 0.02 unit/mL human recombinant AChE or human serum BChE (Sigma Chemical), and 550 $\mu$M substrate (acetylthiocholine iodide or butyrylthiocholine iodide). Test compounds were added to the assay solution and preincubated at 37 °C with the enzyme for 20 min followed by the addition of substrate. Assays were done with a blank containing all components except AChE or BChE to account for nonenzymatic reaction. The reaction rates were compared, and the percentage of inhibition due to the presence of test compounds was calculated. Each concentration was analyzed in triplicate, and $IC_{50}$ values were determined graphically from log concentration−inhibition curves.

**Determination of the Inhibitory Effect on A$\beta$ Aggregation Induced by AChE**. Aliquots of 2 $\mu$L of A$\beta$(1−40) (Bachem AG, Switzerland), lyophilized from 2 mg/mL HFIP and dissolved in DMSO at a final concentration of 230 $\mu$M, were incubated for 24 h at room temperature in 0.215 M sodium phosphate buffer (pH 8.0). For coincubation experiments, aliquots of AChE (2.30 $\mu$M, ratio 100:1) and AChE in the presence of the tested compound (100 $\mu$M) were added. Blanks containing A$\beta$, AChE, A$\beta$ plus the tested compound, and AChE plus the tested compound in 0.215 M sodium phosphate buffer (pH 8.0) were prepared. The final volume of each vial was 20 $\mu$L. To quantify amyloid fibril formation, the thioflavin T fluorescence method was used.[32,33,55] Thioflavin T binds to amyloid fibrils, giving rise to an intense specific emission band at 490 nm in its fluorescent emission spectrum. Therefore, after incubation, the samples were diluted to a final volume of 2 mL with 50 mM glycine−NaOH buffer (pH 8.5) containing 1.5 $\mu$M thioflavin T. A 300 s time scan of fluorescence intensity was carried out ($\lambda_{exc}$ = 446 nm, $\lambda_{em}$ = 490 nm), and values at the plateau were averaged after subtraction of the background fluorescence of the 1.5 $\mu$M thioflavin T solution.

**Determination of the Inhibitory Effect on the Self-Mediated A$\beta$(1−42) Aggregation**. To investigate the self-mediated A$\beta$(1−42) aggregation, a thioflavin T based fluorometric assay was performed. HFIP-pretreated A$\beta$(1−42) samples (Bachem AG) were resolubilized with a $CH_3CN/Na_2CO_3$/NaOH (48.4:48.4:3.2) to have a stable stock solution ([A$\beta$] = 500 $\mu$M). Experiments were performed by incubating the peptide in 10 mM phosphate buffer (pH 8.0) containing 10 mM NaCl at 30 °C for 24 h (final A$\beta$ concentration 50 $\mu$M) with and without the tested compound at 10 $\mu$M. To quantify amyloid fibril formation, the thioflavin T fluorescence method was used.[32,33,55] After incubation, the samples were diluted to a final volume of 2.0 mL with 50 mM glycine−NaOH buffer (pH 8.5) containing 1.5 $\mu$M thioflavin T. A 300 s time scan of fluorescence intensity was carried out ($\lambda_{exc}$ = 446 nm, $\lambda_{em}$ = 490 nm), and values at the plateau were averaged after subtraction of the background fluorescence of the 1.5 $\mu$M thioflavin T solution.

**Determination of Antioxidant Activity in SH-SY5Y Cells**. Human neuronal-like cells, SH-SY5Y, were routinely grown at 37 °C in a humidified incubator with 5% $CO_2$ in Dulbecco's modified Eagle's medium supplemented with 10% fetal calf serum (FCS), 2 mM glutamine, 50 U/mL penicillin, and 50 $\mu$g/mL streptomycin. To evaluate the antioxidant activity of the compounds, SH-SY5Y cells were seeded in 96-well plates at 3 × 10$^4$ cells/well. Experiments were performed after 24 h of incubation at 37 °C in 5% $CO_2$ with 4-methylsulfinylbutyl isothiocyanate (2.5 $\mu$M), a potent inducer of cytosolic NQO1. The antioxidant activity of compounds **2**, **5**, and **8** was evaluated using a fluorescent probe (2′,7′-dichlorofluorescein diacetate, DCFH-DA), by measuring the intracellular ROS formation evoked by exposure of SH-SY5Y cells to *tert*-butyl hydroperoxide (*t*-BuOOH), a compound used to induce oxidative stress.[36] After 24 h of treatment with the compounds, the SH-SY5Y cells were washed with PBS and then incubated with 5 $\mu$M DCFH-DA in PBS at 37 °C in 5% $CO_2$ for 30 min. After removal of DCFH-DA and further washing, the cells were incubated with 0.1 mM *t*-BuOOH in PBS for 30 min. At the end of incubation, the fluorescence of the cells from each well was measured ($\lambda_{exc}$ = 485 nm, $\lambda_{em}$ = 535 nm) with a spectrofluorometer (Wallac Victor multilabel counter, Perkin-Elmer Inc., Boston, MA). The results are expressed as the percentage increase of intracellular ROS evoked by exposure to *t*-BuOOH and calculated by the formula $[(F_t - F_{nt})/F_{nt} \times 100]$, where $F_t$ = fluorescence of treated neurones and $F_{nt}$ = fluorescence of untreated neurones.

Data are reported as the mean ± SD of at least three independent experiments. Statistical analysis was performed using ANOVA (the Scheffe post hoc test was used), and the differences were considered significant at $p < 0.05$. Analyses were performed using STATISTICA 4.5 software on a Windows platform.

**Substrate Specificity for NQO1**. **2**, **5**, and **8** were tested with respect to their ability to accept electrons from NADH via human NQO1 (Sigma), by following the absorbance change of NADH. Menadione was used as a reference compound. Briefly, each reaction consisted of NADH, NQO1, and the tested compounds in a final volume of Tris−HCl buffer containing bovine serum albumin (0.07%). Reactions were started by the addition of NADH. The time course of the reaction was followed by monitoring the absorbance decrease of NADH at 340 nm, using an extinction coefficient of 6.22 $mM^{-1}$ $cm^{-1}$ in a Jasco 7850 double-beam spectrophotometer. The extent of nonenzymatic quinone reduction by NADH was determined in all cases either in the absence of the enzyme or in the presence of 20 $\mu$M dicoumarol. The results are expressed in terms of the apparent $V_{max}$ and $K_m$ for three independent titrations.

**Computational Studies**. The 3D models of compounds **2**, **7**, **8**, and **10** were built using Sybyl 7.1.1 (Tripos Associates, Inc., St. Louis, MO, 2001) and geometry optimized at the density functional level of theory (B3LYP/6-31G*) by means of the software Gaussian03.[56] Docking simulations were carried out by means of the GOLD software[38] (v. 3.0.1) and using the crystal structure of human AChE in complex with fasciculin (PDB code 1B41).[39] Fasciculin was removed, and the ligand binding site was defined at 10 Å from the oxygen of the Tyr124 side chain. As suggested by the GOLD authors,[38] genetic algorithm default parameters were set: the population size was 100, the selection pressure was 1.1, the number of operations was $10^5$, the number of islands was 5, the niche size was 2, migrate was 10, mutate was 95, and crossover was 95. A total of 100 poses were generated by GOLD and then clusterized by means of AClAP (v. 1.0).[40,41] Briefly, AClAP is a newly developed clustering protocol implemented in a MATLAB metalanguage program, which combines a hierarchical agglomerative cluster analysis with a clusterability assessment method and a user-independent cutting rule.[41] In particular, when applied to docking outcomes, we demonstrated that the combination of the average linkage rule with the cutting function developed by Sutcliffe and co-workers[57] turned out to be an approach that meets all the criteria required for a robust clustering protocol.[40] The pose reported in Figure 2 for compounds **7**, **8**, and **10** is a low-energy conformation representative of the most populated cluster that, according to the Chauvenet criterion,[40,41] was statistically populated. Concerning **2**, the pose representative of the most populated cluster was used as the starting conformation for subsequent molecular dynamics simulations.

The binary complex between AChE and **2** was investigated by means of MD simulations carried out with the AMBER 8.0 package software.[42] Seven nanosecond MD simulations on the **2**−hAChE binary complex were carried out in explicit solvent and periodic boundary conditions. Six $Na^+$ counterions were added to the solvent bulk of the protein−water complexes to maintain neutrality in the systems. First, water shells and counterions were minimized using

steepest descent and conjugate gradient algorithms. Then a minimization of the entire ensemble was performed setting a convergence criterion on the gradient of 0.001 kcal $mol^{-1}$ $Å^{-1}$. Then equilibration runs were carried out by heating the system to 300 K in 100 ps. This was followed by 7 ns MD simulations in the NPT ensemble (constant temperature and pressure). The parm99 version[58] of the all-atom Amber force field[59] was used for the protein and the counterions, whereas the TIP3P model[60] was employed to explicitly represent water molecules. van der Waals and short-range electrostatic interactions were estimated within a 10 Å cutoff, whereas the long-range electrostatic interactions were assessed by using the particle mesh Ewald (PME) method,[61] with a ~1 Å charge grid spacing interpolated by a fourth-order B-spline, and by setting the direct sum tolerance to $10^{-5}$. Bonds involving hydrogen atoms were constrained by using the SHAKE algorithm[62] with a relative geometric tolerance for coordinate resetting of 0.00001 Å. Berendsen's coupling algorithms[63] were employed to maintain constant temperature and pressure with the same scaling factor for both solvent and solutes and with the time constant for heat bath coupling maintained at 1.5 ps. The pressure for the isothermal−isobaric ensemble was regulated by using a pressure relaxation time of 1 ps in Berendsen's algorithm. The simulations of the solvated protein models were performed using a constant pressure of 1 atm and a constant temperature of 300 K.

All calculations were performed on a Linux cluster employing an openMosix architecture.

**Acknowledgment.** This research was supported by a grant from MIUR (FIRB RBNE03FH5Y), the University of Bologna, and Lay Line Genomics.

**Supporting Information Available:** Elemental analysis results for target compounds, chemical structures of reference compounds, and NMR data for intermediate compounds. This material is available free of charge via the Internet at http://pubs.acs.org.

## References

(1) Bartus, R. T.; Dean, R. L., III; Beer, B.; Lippa, A. S. The cholinergic hypothesis of geriatric memory dysfunction. *Science* **1982**, *217*, 408−414.
(2) Terry, A. V., Jr.; Buccafusco, J. J. The cholinergic hypothesis of age and Alzheimer's disease-related cognitive deficits: recent challenges and their implications for novel drug development. *J. Pharmacol. Exp. Ther.* **2003**, *306*, 821−827.
(3) Cummings, J. L. Treatment of Alzheimer's disease: current and future therapeutic approaches. *Rev. Neurol. Dis.* **2004**, *1*, 60−69.
(4) McLaurin, J.; Kierstead, M. E.; Brown, M. E.; Hawkes, C. A.; Lambermon, M. H.; Phinney, A. L.; Darabie, A. A.; Cousins, J. E.; French, J. E.; Lan, M. F.; Chen, F.; Wong, S. S.; Mount, H. T.; Fraser, P. E.; Westaway, D.; St George-Hyslop, P. Cyclohexanehexol inhibitors of Abeta aggregation prevent and reverse Alzheimer phenotype in a mouse model. *Nat. Med.* **2006**, *12*, 801−808.
(5) Khlistunova, I.; Biernat, J.; Wang, Y.; Pickhardt, M.; von Bergen, M.; Gazova, Z.; Mandelkow, E.; Mandelkow, E. M. Inducible expression of Tau repeat domain in cell models of tauopathy: aggregation is toxic to cells but can be reversed by inhibitor drugs. *J. Biol. Chem.* **2006**, *281*, 1205−1214.
(6) Hardy, J.; Duff, K.; Hardy, K. G.; Perez-Tur, J.; Hutton, M. Genetic dissection of Alzheimer's disease and related dementias: amyloid and its relationship to tau. *Nat. Neurosci.* **1998**, *1*, 355−358.
(7) Youdim, M. B.; Buccafusco, J. J. Multi-functional drugs for various CNS targets in the treatment of neurodegenerative disorders. *Trends Pharmacol. Sci.* **2005**, *26*, 27−35.
(8) Youdim, M. B.; Buccafusco, J. J. CNS Targets for multi-functional drugs in the treatment of Alzheimer's and Parkinson's diseases. *J. Neural Transm.* **2005**, *112*, 519−537.
(9) Csermely, P.; Agoston, V.; Pongor, S. The efficiency of multi-target drugs: the network approach might help drug design. *Trends Pharmacol. Sci.* **2005**, *26*, 178−182.
(10) Espinoza-Fonseca, L. M. The benefits of the multi-target approach in drug design and discovery. *Bioorg. Med. Chem.* **2006**, *14*, 896−897.
(11) Rosini, M.; Andrisano, V.; Bartolini, M.; Bolognesi, M. L.; Hrelia, P.; Minarini, A.; Tarozzi, A.; Melchiorre, C. Rational approach to discover multipotent anti-Alzheimer drugs. *J. Med. Chem.* **2005**, *48*, 360−363.
(12) Bolognesi, M. L.; Minarini, A.; Tumiatti, V.; Melchiorre, C. Lipoic acid, a lead structure for multi-target-directed drugs for neurodegeneration. *Mini Rev. Med. Chem.* **2006**, *6*, 1269−1274.
(13) Nunomura, A.; Perry, G.; Aliev, G.; Hirai, K.; Takeda, A.; Balraj, E. K.; Jones, P. K.; Ghanbari, H.; Wataya, T.; Shimohama, S.; Chiba, S.; Atwood, C. S.; Petersen, R. B.; Smith, M. A. Oxidative damage is the earliest event in Alzheimer disease. *J. Neuropathol. Exp. Neurol.* **2001**, *60*, 759−767.
(14) Hopkins, A. L.; Mason, J. S.; Overington, J. P. Can we rationally design promiscuous drugs? *Curr. Opin. Struct. Biol.* **2006**, *16*, 127−136.
(15) Melchiorre, C.; Angeli, P.; Brasili, L.; Giardinà, D.; Pigini, M.; Quaglia, W. Polyamines: a possible "passe-partout" for receptor characterization. *Actual. Chim. Thér., 15e Sér.* **1988**, 149−168.
(16) Bolognesi, M. L.; Minarini, A.; Budriesi, R.; Cacciaguerra, S.; Chiarini, A.; Spampinato, S.; Tumiatti, V.; Melchiorre, C. Universal template approach to drug design: polyamines as selective muscarinic receptor antagonists. *J. Med. Chem.* **1998**, *41*, 4150−4160.
(17) Melchiorre, C.; Andrisano, V.; Bolognesi, M. L.; Budriesi, R.; Cavalli, A.; Cavrini, V.; Rosini, M.; Tumiatti, V.; Recanatini, M. Acetylcholinesterase noncovalent inhibitors based on a polyamine backbone for potential use against Alzheimer's disease. *J. Med. Chem.* **1998**, *41*, 4186−4189.
(18) Beal, M. F. Mitochondrial dysfunction and oxidative damage in Alzheimer's and Parkinson's diseases and coenzyme Q10 as a potential treatment. *J. Bioenerg. Biomembr.* **2004**, *36*, 381−386.
(19) Bragin, V.; Chemodanova, M.; Dzhafarova, N.; Bragin, I.; Czerniawski, J. L.; Aliev, G. Integrated treatment approach improves cognitive function in demented and clinically depressed patients. *Am. J. Alzheimer's Dis. Other Dementias* **2005**, *20*, 21−26.
(20) Ono, K.; Hasegawa, K.; Naiki, H.; Yamada, M. Preformed beta-amyloid fibrils are destabilized by coenzyme Q10 in vitro. *Biochem. Biophys. Res. Commun.* **2005**, *330*, 111−116.
(21) Tomiyama, T.; Shoji, A.; Kataoka, K.; Suwa, Y.; Asano, S.; Kaneko, H.; Endo, N. Inhibition of amyloid beta protein aggregation and neurotoxicity by rifampicin. Its possible function as a hydroxyl radical scavenger. *J. Biol. Chem.* **1996**, *271*, 6839−6844.
(22) Tumiatti, V.; Andrisano, V.; Banzi, R.; Bartolini, M.; Minarini, A.; Rosini, M.; Melchiorre, C. Structure-activity relationships of acetylcholinesterase noncovalent inhibitors based on a polyamine backbone. 3. Effect of replacing the inner polymethylene chain with cyclic moieties. *J. Med. Chem.* **2004**, *47*, 6490−6498.
(23) Cavalli, A.; Bolognesi, M. L.; Capsoni, S.; Andrisano, V.; Bartolini, M.; Margotti, E.; Cattaneo, A.; Recanatini, M.; Melchiorre, C. A small molecule targeting the multifactorial nature of Alzheimer's disease. *Angew. Chem., Int. Ed.* **2007**, *46*, 3689−3692.
(24) Nesterov, E. E.; Skoch, J.; Hyman, B. T.; Klunk, W. E.; Bacskai, B. J.; Swager, T. M. In vivo optical imaging of amyloid aggregates in brain: design of fluorescent markers. *Angew. Chem., Int. Ed.* **2005**, *44*, 5452−5456.
(25) Gribble, G. W.; Jasinski, J. M.; Pellicone, J. T.; Panetta, J. A. N-Alkylation of aliphatic secondary amines with carboxylic acids. *Synthesis* **1998**, 766−768.
(26) Dubowchik, G. M.; Michne, J. A.; Zuev, D. An efficient sequence for the preparation of small secondary amine hydrochloride salts for focused library generation without need for distillation or chromatographic purification. *Bioorg. Med. Chem. Lett.* **2004**, *14*, 3147−3149.
(27) Bolognesi, M. L.; Bixel, M. G.; Marucci, G.; Bartolini, M.; Krauss, M.; Angeli, P.; Antonello, A.; Rosini, M.; Tumiatti, V.; Hucho, F.; Melchiorre, C. Structure-activity relationships of methoctramine-related polyamines as muscular nicotinic receptor noncompetitive antagonists. 3. Effect of inserting the tetraamine backbone into a macrocyclic structure. *J. Med. Chem.* **2002**, *45*, 3286−3295.
(28) Piazzi, L.; Belluti, F.; Bisi, A.; Gobbi, S.; Rizzo, S.; Bartolini, M.; Andrisano, V.; Recanatini, M.; Rampa, A. Cholinesterase inhibitors: SAR and enzyme inhibitory activity of 3-[omega-(benzylmethylamino)alkoxy]xanthen-9-ones. *Bioorg. Med. Chem.* **2007**, *15*, 575−585.
(29) Inestrosa, N. C.; Alvarez, A.; Calderon, F. Acetylcholinesterase is a senile plaque component that promotes assembly of amyloid beta-peptide into Alzheimer's filaments. *Mol. Psychiatry* **1996**, *1*, 359−361.
(30) Bartolini, M.; Bertucci, C.; Cavrini, V.; Andrisano, V. beta-Amyloid aggregation induced by human acetylcholinesterase: inhibition studies. *Biochem. Pharmacol.* **2003**, *65*, 407−416.
(31) Dickerson, T. J.; Beuscher, A. E. t.; Rogers, C. J.; Hixon, M. S.; Yamamoto, N.; Xu, Y.; Olson, A. J.; Janda, K. D. Discovery of acetylcholinesterase peripheral anionic site ligands through computational refinement of a directed library. *Biochemistry* **2005**, *44*, 14845−14853.
(32) Naiki, H.; Higuchi, K.; Nakakuki, K.; Takeda, T. Kinetic analysis of amyloid fibril polymerization in vitro. *Lab. Invest.* **1991**, *65*, 104−110.

(33) LeVine, H., 3rd Thioflavine T interaction with synthetic Alzheimer's disease beta-amyloid peptides: detection of amyloid aggregation in solution. *Protein Sci.* **1993**, *2*, 404−410.
(34) Datki, Z.; Papp, R.; Zadori, D.; Soos, K.; Fulop, L.; Juhasz, A.; Laskay, G.; Hetenyi, C.; Mihalik, E.; Zarandi, M.; Penke, B. In vitro model of neurotoxicity of Abeta 1−42 and neuroprotection by a pentapeptide: irreversible events during the first hour. *Neurobiol. Dis.* **2004**, *17*, 507−515.
(35) Mordente, A.; Martorana, G. E.; Minotti, G.; Giardina, B. Antioxidant properties of 2,3-dimethoxy-5-methyl-6-(10-hydroxydecyl)-1,4-benzoquinone (idebenone). *Chem. Res. Toxicol.* **1998**, *11*, 54−63.
(36) Wang, H.; Joseph, J. A. Quantifying cellular oxidative stress by dichlorofluorescein assay using microplate reader. *Free Radical Biol. Med.* **1999**, *27*, 612−616.
(37) Fahey, J. W.; Zhang, Y.; Talalay, P. Broccoli sprouts: an exceptionally rich source of inducers of enzymes that protect against chemical carcinogens. *Proc. Natl. Acad. Sci. U.S.A.* **1997**, *94*, 10367−10372.
(38) Jones, G.; Willett, P.; Glen, R. C.; Leach, A. R.; Taylor, R. Development and validation of a genetic algorithm for flexible docking. *J. Mol. Biol.* **1997**, *267*, 727−748.
(39) Kryger, G.; Harel, M.; Giles, K.; Toker, L.; Velan, B.; Lazar, A.; Kronman, C.; Barak, D.; Ariel, N.; Shafferman, A.; Silman, I.; Sussman, J. L. Structures of recombinant native and E202Q mutant human acetylcholinesterase complexed with the snake-venom toxin fasciculin-II. *Acta Crystallogr., D: Biol. Crystallogr.* **2000**, *56*, 1385−1394.
(40) Bottegoni, G.; Cavalli, A.; Recanatini, M. A comparative study on the application of hierarchical-agglomerative clustering approaches to organize outputs of reiterated docking runs. *J. Chem. Inf. Model* **2006**, *46*, 852−862.
(41) Bottegoni, G.; Rocchia, W.; Recanatini, M.; Cavalli, A. AClAP, Autonomous hierarchical agglomerative Cluster Analysis based protocol to partition conformational datasets. *Bioinformatics* **2006**, *22*, e58−65.
(42) Case, D. A.; Darden, T. E.; Cheatham, T. E. I.; Simmerling, C. L.; Wang, J.; Duke, R. E.; Luo, R.; Merz, K. M.; Wang, B.; Pearlman, D. A.; Crowley, M.; Brozell, S.; Tsui, V.; Gohlke, H.; Mongan, J.; Hornak, V.; Cui, G.; Beroza, P.; Schafmeister, C.; Caldwell, J. W.; Ross, W. S.; Kollman, P. A. *AMBER 8*; University of California: San Francisco.
(43) Tumiatti, V.; Rosini, M.; Bartolini, M.; Cavalli, A.; Marucci, G.; Andrisano, V.; Angeli, P.; Banzi, R.; Minarini, A.; Recanatini, M.; Melchiorre, C. Structure-activity relationships of acetylcholinesterase noncovalent inhibitors based on a polyamine backbone. 2. Role of the substituents on the phenyl ring and nitrogen atoms of caproctamine. *J. Med. Chem.* **2003**, *46*, 954−966.
(44) Giacobini, E.; Spiegel, R.; Enz, A.; Veroff, A. E.; Cutler, N. R. Inhibition of acetyl- and butyryl-cholinesterase in the cerebrospinal fluid of patients with Alzheimer's disease by rivastigmine: correlation with cognitive benefit. *J. Neural Transm.* **2002**, *109*, 1053−1065.
(45) Diamant, S.; Podoly, E.; Friedler, A.; Ligumsky, H.; Livnah, O.; Soreq, H. Butyrylcholinesterase attenuates amyloid fibril formation in vitro. *Proc. Natl. Acad. Sci. U.S.A.* **2006**, *103*, 8628−8633.
(46) Campiani, G.; Fattorusso, C.; Butini, S.; Gaeta, A.; Agnusdei, M.; Gemma, S.; Persico, M.; Catalanotti, B.; Savini, L.; Nacci, V.; Novellino, E.; Holloway, H. W.; Greig, N. H.; Belinskaya, T.; Fedorko, J. M.; Saxena, A. Development of molecular probes for the identification of extra interaction sites in the mid-gorge and peripheral sites of butyrylcholinesterase (BuChE). Rational design of novel, selective, and highly potent BuChE inhibitors. *J. Med. Chem.* **2005**, *48*, 1919−1929.
(47) Recanatini, M.; Valenti, P. Acetylcholinesterase inhibitors as a starting point towards improved Alzheimer's disease therapeutics. *Curr. Pharm. Des.* **2004**, *10*, 3157−3166.
(48) Bolognesi, M. L.; Andrisano, V.; Bartolini, M.; Banzi, R.; Melchiorre, C. Propidium-based polyamine ligands as potent inhibitors of acetylcholinesterase and acetylcholinesterase-induced amyloid-beta aggregation. *J. Med. Chem.* **2005**, *48*, 24−27.
(49) Rees, T.; Hammond, P. I.; Soreq, H.; Younkin, S.; Brimijoin, S. Acetylcholinesterase promotes beta-amyloid plaques in cerebral cortex. *Neurobiol. Aging* **2003**, *24*, 777−787.
(50) Abe, K.; Kato, M.; Saito, H. Congo red reverses amyloid beta protein-induced cellular stress in astrocytes. *Neurosci. Res.* **1997**, *29*, 129−134.
(51) Beyer, R. E.; Segura-Aguilar, J.; Di Bernardo, S.; Cavazzoni, M.; Fato, R.; Fiorentini, D.; Galli, M. C.; Setti, M.; Landi, L.; Lenaz, G. The role of DT-diaphorase in the maintenance of the reduced antioxidant form of coenzyme Q in membrane systems. *Proc. Natl. Acad. Sci. U.S.A.* **1996**, *93*, 2528−2532.
(52) SantaCruz, K. S.; Yazlovitskaya, E.; Collins, J.; Johnson, J.; DeCarli, C. Regional NAD(P)H:quinone oxidoreductase activity in Alzheimer's disease. *Neurobiol. Aging* **2004**, *25*, 63−69.
(53) Atwell, G. J.; Denny, W. A. Monoprotection of α,ω-alkanediamines with the N-benzyloxycarbonyl group. *Synthesis* **1984**, 1032−1033.
(54) Ellman, G. L.; Courtney, K. D.; Andres, V., Jr.; Feather-Stone, R. M. A new and rapid colorimetric determination of acetylcholinesterase activity. *Biochem. Pharmacol.* **1961**, *7*, 88−95.
(55) Inestrosa, N. C.; Alvarez, A.; Perez, C. A.; Moreno, R. D.; Vicente, M.; Linker, C.; Casanueva, O. I.; Soto, C.; Garrido, J. Acetylcholinesterase accelerates assembly of amyloid-beta-peptides into Alzheimer's fibrils: possible role of the peripheral site of the enzyme. *Neuron* **1996**, *16*, 881−891.
(56) Frisch, M. J.; Trucks, G. W.; Schlegel, H. B.; Scuseria, G. E.; Robb, M. A.; Cheeseman, J. R.; Zakrzewski, V. G.; Montgomery, J. A., Jr.; Stratmann, R. E.; Burant, J. C.; Dapprich, S.; Millam, J. M.; Daniels, A. D.; Kudin, K. N.; Strain, M. C.; Farkas, O.; Tomasi, J.; Barone, V.; Cossi, M.; Cammi, R.; Mennucci, B.; Pomelli, C.; Adamo, C.; Clifford, S.; Ochterski, J.; Petersson, G. A.; Ayala, P. Y.; Cui, Q.; Morokuma, K.; Malick, D. K.; Rabuck, A. D.; Raghavachari, K.; Foresman, J. B.; Cioslowski, J.; Ortiz, J. V.; Stefanov, B. B.; Liu, G.; Liashenko, A.; Piskorz, P.; Komaromi, I.; Gomperts, R.; Martin, R. L.; Fox, D. J.; Keith, T.; Al-Laham, M. A.; Peng, C. Y.; Nanayakkara, A.; Gonzalez, C.; Challacombe, M.; Gill, P. M. W.; Johnson, B. G.; Chen, W.; Wong, M. W.; Andres, J. L.; Head-Gordon, M.; Replogle, E. S.; Pople, J. A. *Gaussian 03*, Revision C.02; Gaussian, Inc.: Pittsburgh, PA.
(57) Kelley, L. A.; Gardner, S. P.; Sutcliffe, M. J. An automated approach for defining core atoms and domains in an ensemble of NMR-derived protein structures. *Protein Eng.* **1997**, *10*, 737−741.
(58) Wang, J.; Cieplak, P.; Kollman, P. A. How well does a restrained electrostatic potential (RESP) model perform in calculating conformational energies of organic and biological molecules? *J. Comput. Chem.* **2000**, *21*, 1049−1074.
(59) Cornell, W. D.; Cieplak, P.; Bayly, C. I.; Gould, I. R.; Merz, K. M.; Ferguson, D. M.; Spellmeyer, D. C.; Fox, T.; Caldwell, J. W.; Kollman, P. A. A second generation force field for the simulation of proteins, nucleic acids, and organic molecules. *J. Am. Chem. Soc.* **1995**, *117*, 5179−5197.
(60) Jorgensen, W. L.; Chandrasekhar, J.; Madura, J. D.; Impey, R. W.; Klein, L. M. Comparison of simple potential functions for simulating liquid water. *J. Chem. Phys.* **1983**, *79*, 926−935.
(61) Essmann, U.; Perera, L.; Berkowitz, M. L.; Darden, T.; Lee, H.; Pedersen, L. G. A smooth particle mesh Ewald method. *J. Chem. Phys.* **1995**, *103*, 8577−8593.
(62) Ryckaert, J. P.; Ciccotti, G.; Berendsen, H. J. C. Numerical integration of the cartesian equations of motion of a system with constraints: molecular dynamics of n-alkanes. *J. Comput. Phys.* **1977**, *23*, 327−341.
(63) Berendsen, H. J. C.; Postma, J. P. M.; Van, Gunsteren, W. F.; Di, Nola, A.; Haak, J. R. Molecular dynamics with coupling to an external bath. *J. Chem. Phys.* **1984**, *81*, 3684−3690.

JM070559A